


Article

Geological Controls on Mineralogical Characteristic Differences of Coals from the Main Coal Fields in Shaanxi, North China

Wei Yuan ^{1,2}, Jing Li ^{1,*} , Xinguo Zhuang ¹, Guanghua Yang ³ and Lei Pan ³

¹ Key Laboratory of Tectonics and Petroleum Resources, China University of Geosciences, Ministry of Education, Lumo Road 388, Wuhan 430074, China; yuanweicumt@126.com (W.Y.); xgzhuang@cug.edu.cn (X.Z.)

² Inner Mongolia Geology Engineering Co., Ltd., Xinhudong Street 87, Hohhot 010010, China

³ Xi'an Institute of Geology and Mineral Exploration, Western Duling Road 56, Xi'an 710100, China; Fushiaihua1999@sina.com (G.Y.); panlei@snjwx.com (L.P.)

* Correspondence: jingli@cug.edu.cn

Abstract: Shaanxi is among the provinces with abundant coal resources in North China. These enormous coal resources (approx. 4143 Gt) are widely distributed in the Ordos Basin and its marginal fold belts. The main coal-bearing strata consist of the late Carboniferous Taiyuan Formation, the early Permian Shanxi Formation, the late Triassic Wayaobao Formation, and the middle Jurassic Yan'an Formation, which were respectively deposited in coastal plains and a lagoon environment, a continental environment, an inland open lake and a confined lake environment. The Permo-Carboniferous coals are low volatile bituminous and characterized by relatively high vitrinite content, which decreases from south to north, and from the lower coal seams upwards. By contrast, the late Triassic and middle Jurassic coals are highly volatile bituminous, but are respectively characterized by relatively high vitrinite and high inertinite content. Minerals in the Permo-Carboniferous coals, the late Triassic coals, and the middle Jurassic coals, are respectively dominated by kaolinite and calcite, quartz and kaolinite, and quartz and calcite. Furthermore, contemporary coals deposited in different coal fields or even different mines of the same coal field present different mineral characteristics. The Permian Shanxi Formation coals from the Shanbei C-P coalfield in the north of Shaanxi Province are characterized by higher kaolinite and lower carbonate contents compared to those from the Weibei C-P coalfield in the south of Shaanxi Province. The distinctive mineralogical characteristics of coals formed in different coalfields and different geological ages were ascribed to integrated influences of different terrigenous detrital input from sediment provenance, sedimentary settings (e.g., subsidence rate, sea transgression, and regression process), and hydrothermal activities.

Keywords: minerals in coals; sediment provenance; subsidence rate; sea transgression and regression; hydrothermal influence; different coalfields in Shaanxi Province



Citation: Yuan, W.; Li, J.; Zhuang, X.; Yang, G.; Pan, L. Geological Controls on Mineralogical Characteristic Differences of Coals from the Main Coal Fields in Shaanxi, North China. *Energies* **2021**, *14*, 7905. <https://doi.org/10.3390/en14237905>

Academic Editor: Maxim Tyulenev

Received: 28 October 2021

Accepted: 19 November 2021

Published: 25 November 2021

Publisher's Note: MDPI stays neutral with regard to jurisdictional claims in published maps and institutional affiliations.



Copyright: © 2021 by the authors. Licensee MDPI, Basel, Switzerland. This article is an open access article distributed under the terms and conditions of the Creative Commons Attribution (CC BY) license (<https://creativecommons.org/licenses/by/4.0/>).

1. Introduction

As an important part of the Ordos Basin, Shaanxi Province has become one of the most significant bases for coal resource exploitation in China, with estimated coal reserves of approx. 4143 Gt [1]. The coal production from both underground and open pit mines is slightly increasing every year, attaining 6.79 Gt in 2020, which has been mainly utilized for electric and heat power generation, coal chemical industry [1]. According to the geological age and the geographic distribution, there are dominantly five important coalfields in Shaanxi Province, comprising two Permo-Carboniferous (Weibei and Shanbei), one Triassic (Shanbei), and two Jurassic (Huanglong and Shanbei) coalfields (Figure 1). Due to the different tectonic evolution stages and deposition conditions, mineralogical and geochemical characteristics of coals vary remarkably among these coal fields [2–7].

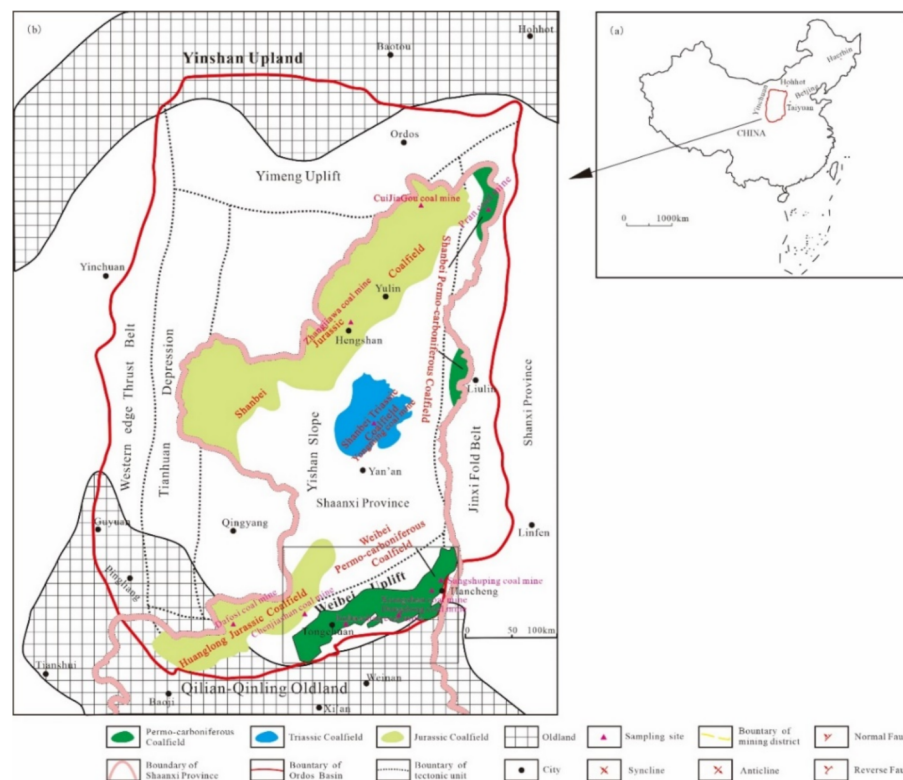


Figure 1. Distribution of the main coal fields in Shaanxi Province and locations of sampling sites (modified after Wang et al., 2011 [4]). (a) Location of Ordos basin; (b) distribution of the main coal fields and locations of sampling sites in Shaanxi Province.

The composition, abundance, distribution, and modes of occurrence of minerals in coals may provide significant geologic information on coal depositional conditions, coal-bearing sequence formation, regional geological history, and associated diagenetic and epigenetic processes affecting coal formation [8–19]. Furthermore, minerals may significantly affect the utilization of coal, from mining and grinding to combustion, gasification and liquefaction technological problems, from coal cleaning to waste disposal, and from environmental impacts to human health consequences [13,16,17,20–24]. In particular, typical mineral phases are important carriers of critical elements (e.g., Ga, Li, Zr, Hf, Nb, Ta, rare earth elements and Y, etc.) and toxic elements (e.g., S, As, F, Hg) in coal [13,21,25–28]. Therefore, research on coal mineralogy is of great significance for possible pollution control of toxic trace elements, for potential recovery of critical elements during coal combustion and utilization, and for other integrated utilization of coals from both an environmental and economic point of view.

Several studies have been conducted on the elemental and mineralogical characteristics of coal seams in the Ordos Basin, with special emphasis on the geochemical characteristics of hazardous elements (S, As, Hg, and Se) [2,3,29–32], and potential critical elements (Ga, Li, Ge, Nb, Zr, and REY) in coals from several coal basins in the Ordos Basin [4,6,7,33–37]. However, as important carriers of critical elements, the geological controls on distribution, occurrence, and origin of minerals in coal are still not clear. To a large extent, this restricts the integrated utilization of the enormous coal resources in Ordos Basin. The present research focused on the main coalfields in Shaanxi Province, and investigated the differences in composition, abundance, modes of occurrence, and distribution of minerals in coals from these coalfields, aiming to investigate the origins and geological factors that may have controlled the mineralogical characteristic differences of coals from different coalfields and different geological ages. The findings in this research will provide important geological and genetic implication of typical minerals in contempo-

aneous coal seams, and further contribute to identifying the occurrence or enrichment of potential critical or hazardous elements in typical minerals.

2. Geological Setting

The coal fields in Shaanxi Province are largely distributed in the Ordos Basin (Figure 1), which is a large complex craton basin superimposed on the Paleozoic North China craton and has undergone a series of tectonic movements, gradually evolving from the early Paleozoic marginal sea basin, the late Carboniferous-middle Triassic intracraton basin, and the late Triassic-early Cretaceous remnant craton basin, to the current intracontinental depression basin [38].

The coal-bearing strata primarily consist of the late Carboniferous Taiyuan Formation, the early Permian Shanxi formation, the late Triassic Wayaobao Formation, and the middle Jurassic Yan'an Formation (Figures 2–4). The Taiyuan Formation continuously overlies the late Carboniferous Benxi Formation and mainly consists of sandstones, mudstones, limestones, muddy limestones, sideritic shales, claystones, and coal seams (Nos. 5–11 coals), among which the No. 5 coal seam is the major minable seam and is 2.5 m thick on average. Continuously overlying the Taiyuan Formation, the Shanxi Formation is composed of sandstone, mudstone, and four thin and discontinuous coal seams (Nos. 1–4 coals) (Figure 2).

The late Triassic Wayaobao Formation parallel-unconformably underlies the early Jurassic Fuxian Formation, and continuously overlies the late Triassic Yongping Formation (Figure 3). The Wayaobao Formation is subdivided into five members from bottom to top, and the lower four members are mainly composed of sandstone, mudstone, and several coal seams, whereas the upper 5th member is composed of oil shale interbedded with bauxitic mudstone and coal seams [39].

The middle Jurassic Yan'an Formation continuously overlies the Fuxian Formation and underlies the Zhiluo Formation, and is also subdivided into five members (Figure 4). The lower first member is composed of conglomeratic sandstone in the lower portion, and of siltstone, mudstone, and coal seams (No. 5) in the upper portion. The upper four members are composed of interbedded sandstone, mudstone, and coal seams (Nos. 1–4).

The coal fields were deposited on the early Paleozoic weathered basement, and have been subjected to sea transgression since the late Carboniferous. The lower member of the late Carboniferous Taiyuan Formation was primarily deposited in a confined epicontinental sedimentary system, during which the Weibei Permo-Carboniferous coalfield was mainly formed in a floodplain, confined carbonate platform, and tidal flat environment [40]. During the second and the upper member of the Taiyuan Formation period, the whole Ordos Basin experienced the maximum transgression, and was mainly deposited in an open epicontinental and bay-lagoon sedimentary system. In particular, the areas in the south of Yulin City were largely deposited in a carbonate platform, and the Weibei Permo-Carboniferous coalfield in the southern margin was partly deposited in a banded tidal flat, the sediment source of which was derived from the south; whereas the Shanbei Permo-Carboniferous coalfield in the north of Yulin City was mainly deposited in a floodplain and the sediment source was derived from the north. Due to the influence of Hercynian tectonic movement and corresponding regression of sea water from the east and west, the early Permian Formation area was predominantly deposited in a continental delta and lake sedimentary system. Due to the differential subsidence rate of the northern and southern part, the former, having a slow subsidence rate, was mainly developed in alluvial and continental delta sedimental facies, whereas the latter, having a rapid slow subsidence rate, was predominantly formed in lacustrine sedimentary facies.

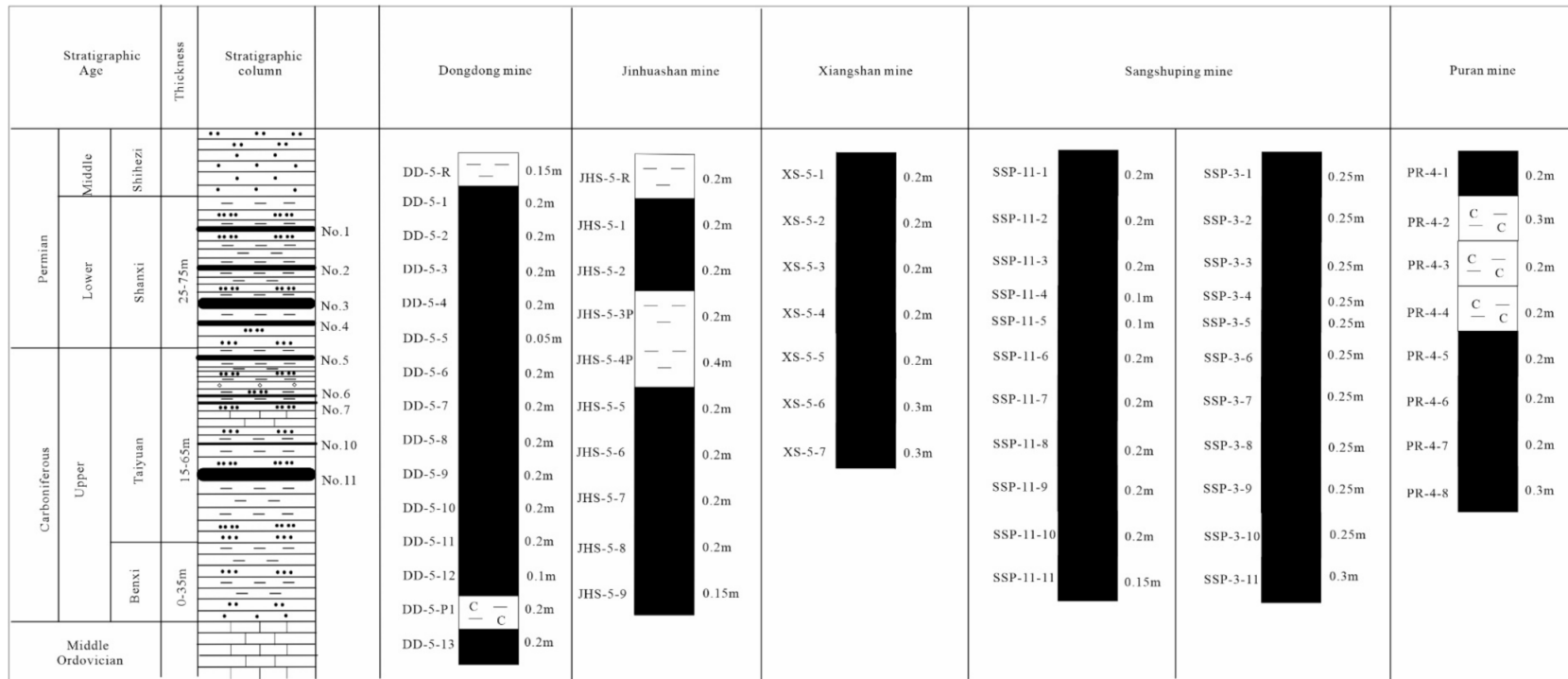


Figure 2. The Late Carboniferous-early Permian coal-bearing stratigraphic column of Shaanxi Province.

System	Formation	Thickness	Sampling column	Yongming mine	
Jurassic	Fuxian Formation				
Late Triassic	Wayobao formation	30m			
		50m		YM-3-01 0.15m	YM-5-01 0.20m
				YM-3-02 0.15m	YM-5-02 0.20m
				YM-3-03 0.15m	YM-5-03 0.20m
				YM-3-04 0.25m	YM-5-04 0.15m
				YM-5-05 0.20m	
50m			YM-5-06 0.20m		
50m			YM-5-07 0.20m		
10m			YM-5-08 0.20m		

Figure 3. The late Triassic coal-bearing stratigraphic column of Shaanxi Province.

System	Formation	Thickness	Sampling column	Cuijiagou mine			Chenjiashan mine			Dafosi mine		Zhangjiawan mine		
Middle Jurassic	Zhiluo Formation												
	Yan'an Formation	2-35m												
		1-40m	CJG-1-01	0.3m	CJG-2-01	0.3m	CJG-3-01	0.3m	CJS-4-01	0.15m	DFS-4-01	0.25m	ZJW-3-01	0.20m
			CJG-1-02	0.3m	CJG-2-02	0.3m	CJG-3-02	0.3m	CJS-4-02	0.15m	DFS-4-02	0.25m	ZJW-3-02	0.20m
			CJG-1-03	0.3m	CJG-2-03	0.3m	CJG-3-03	0.3m	CJS-4-03	0.15m	DFS-4-03	0.20m	ZJW-3-03	0.20m
			CJG-1-04	0.3m	CJG-2-04	0.3m	CJG-3-04	0.3m	CJS-4-04	0.15m	DFS-4-04	0.25m	ZJW-3-04	0.20m
			CJG-1-05	0.3m	CJG-2-05	0.3m	CJG-3-05	0.3m	CJS-4-05	0.15m	DFS-4-05	0.25m	ZJW-3-05	0.25m
			CJG-1-06	0.25m	CJG-2-06	0.3m	CJG-3-06	0.3m	CJS-4-06	0.15m	DFS-4-06	0.25m	ZJW-3-06	0.25m
			CJG-1-07	0.25m	CJG-2-07	0.3m			CJS-4-07	0.15m	DFS-4-07	0.25m	ZJW-3-07	0.20m
	CJG-1-08		0.3m	CJG-2-08	0.3m			CJS-4-08	0.15m	DFS-4-08	0.25m	ZJW-3-08	0.20m	
1-70m				CJG-2-09	0.2m			CJS-4-09	0.15m	DFS-4-09	0.25m	ZJW-3-09	0.20m	
								CJS-4-10	0.15m	DFS-4-10	0.30m	ZJW-3-10	0.20m	
								CJS-4-11	0.15m			ZJW-3-11	0.20m	
								CJS-4-12	0.15m			ZJW-3-12	0.20m	
								CJS-4-13	0.15m			ZJW-3-13	0.20m	
								CJS-4-14	0.15m					
3-25m								CJS-4-15	0.15m					
								CJS-4-16	0.15m					
	Fuxian Formation												

Figure 4. The middle Jurassic coal-bearing stratigraphic column of Shaanxi Province.

The late Triassic Wayaobao Formation was formed in a relatively stable tectonic setting and primarily deposited in a continental fluvial, lake, and lake delta sedimentary environment. Laterally, the areas in the north of Hengshan-Jiaxian City were predominantly deposited in a fluvial sedimentary system, which was characterized by coarse-grained sediments, and those in the south were predominantly deposited in lake and lake delta sedimentary systems that were characterized by relatively fine-grained sediments. Vertically, the 1st and 5th member of the Wayaobao Formation was mainly deposited in fluvial sedimentary system, whereas the 2nd, 3rd, and 4th members were mainly in lake and lake delta sedimentary systems. The Shanbei Triassic coalfield was largely formed in a lake and lake delta environment.

The middle Jurassic Yan'an Formation is divided into five members. The 1st member was mainly formed in a confined lacustrine sedimentary system, the 2nd member was deposited in the concurrent sedimentary framework of alluvial, lake, and delta sedimentary systems, and coal seams were partially formed in the peat mire of the delta plain. The 3rd member was deposited in the concurrent sedimentary framework of lake and delta sedimentary systems; during the late period, the lake largely became shallow and the delta was abandoned, on which coal seams were formed and widely distributed. The lake further shrank and retrograded during the deposition of the 4th and 5th members, which were formed in the concurrent sedimentary framework of confined lacustrine and alluvial sedimentary systems.

3. Methodology

A total of one hundred and forty-two coal and non-coal samples were collected from ten underground coal mines in the Shanbei Jurassic, Shanbei Carboniferous-Permian, Shanbei Triassic, Huanglong Jurassic, and Weibei Carboniferous-Permian coalfields (Figure 1). Among these, twenty coal and non-coal rock samples of the early Permian Shanxi Formation (P_{1s}) were obtained from the No. 3 coal seam of the Puran coal mine in the Shanbei Carboniferous-Permian Coalfield and the No. 4 coal seam of the Sangshuping coal mine in the Weibei Carboniferous-Permian Coalfield. Forty-seven coal and non-coal rock samples the Late Carboniferous Taiyuan Formation (C_{2t}) were respectively collected from the No. 5 and No. 11 coal seams of the Dongdong, Jinhushan, Xiangshan, and Sangshuping coal mines of the Weibei Carboniferous-Permian Coalfield (Figure 2). Thirteen coal and non-coal rock samples of the late Triassic Wayaobao Formation (T_{3w}) were collected from the No. 3 and No. 5 coal seams of the Yongming coal mine in the Shanbei Triassic Coalfield (Figure 3). A total of 62 coal and non-coal rock samples of the middle Jurassic Yan'an Formation (J_{2y}) were respectively obtained from Nos. 1–3 coal seams of the Zhangjiawa and Cuijiagou coal mines in the Shanbei Jurassic Coalfield and the No. 4 coal seam of the Dafoshi and Chenjiashan coal mines in the Huanglong Jurassic Coalfield (Figure 4).

Proximate analysis was carried out following the ASTM Standards D3173, D3174, and D3175 [41–43]. The total sulfur and forms of sulfur were analyzed following the ASTM Standards D4239-18a and D2492-02 [44,45]. Vitrinite reflectance was measured according to the ASTM Standard D2798-20 [46]. Mineralogical compositions of the studied samples were analyzed by powder X-ray diffraction (XRD) using a Bruker D8 A25 diffractometer with monochromatic Cu $K\alpha$ radiation, 2 theta range of 4–60°, step size of 0.19°, and counting time of 0.1 s/step. An internal reference method was used to semi-quantify the mineral contents [47]. The morphology and modes of occurrence of minerals were observed by a field emission-scanning electron microscope (FE-SEM, FEI Quanta™ 650 FEG, Thermal Fisher, USA) coupled with an energy dispersive X-ray spectrometer (EDX; Genesis Apex 4, EDAX Inc., Mahwah, NJ, USA).

4. Results

4.1. Standard Coal Characteristics

The results of proximate analysis including moisture content, ash, and volatile matter yields in the coals within the different coalfields are summarized in Table 1. According to

the Chinese Standards MT/T 850-2000 and GB/T 15224.1-2010, and ASTM Standard D388-12 [48–50], coals of the late Carboniferous Taiyuan Formation in the Weibei Carboniferous-Permian coalfield are characterized by low moisture content, low to high ash yield, and low to medium volatile matter yield, belonging to low volatile bituminous (Table 1). Coals of the early Permian Shanxi Formation in the Weibei Carboniferous-Permian coalfield contain low moisture content, low ash yield, and low volatile matter yield; in contrast, the analyzed coal samples from the Shanxi Formation in the Shanbei Carboniferous-Permian coalfield contain low moisture content, high ash yield, and high volatile matter yield (Table 1). Accordingly, the former falls within the low volatile bituminous coal rank, whereas the latter falls within the high-volatile A bituminous rank, which is due to the differential subsidence in the south and north of the eastern Ordos basin during this period. After formation of the late Paleozoic coal seam, the subsidence rate was low in the northern area where the coalification is low, whereas the subsidence rate was high in the southern area where the coalification is high [40].

The Triassic Wayaobao Formation coals generally contain low moisture content, and low to medium ash yields. The volatile matter yield indicates a high-volatile A bituminous coal rank. The No. 3 coal is characterized by lower ash yield compared to the No. 5 coal of the Wayaobao Formation (Table 1).

The middle Jurassic Yan'an Formation coals are predominantly represented by medium moisture content, low ash yield, and high volatile matter yield, pointing to a high-volatile A bituminous coal rank. However, it is worth noting that coals from the Shanbei Jurassic Coalfield contain relatively higher moisture content and volatile matter yield but lower ash yields than the Jurassic coal seams in the Huanglong coalfield. The lateral and vertical variation of coal rank of coal seams formed in different geological ages is mainly attributed to hypozonal metamorphism in the studied area [51].

With respect to the total sulfur content, the late Carboniferous Taiyuan Formation coals from the Weibei C-P coal field are characterized by relatively high S content (avg. 1.8–4.6%), belonging to medium- to high-sulfur coal [52]. The analyzed coal samples from the Sangshuping coal mine of the Weibei coal field are typical superhigh-organic-sulfur (SHOS) coals, with a high proportion of organic sulfur content [6]. The early Permian coal seams in the Shanxi Formation from both the Weibei and Shanbei C-P coalfields are classified as low-sulfur coals. The Triassic and Jurassic coals from the Shanbei and Huanglong coalfields are primarily classified as low-sulfur coals with the exception of some coal samples from the Yan'an Formation in the Shanbei Jurassic coal field (e.g., the Zhangjiawa coal mine), which have relatively high S content. This is consistent with previous research showing that the precursor peats of Jurassic coal seams in the Hengshan and Jingbian areas of the Shanbei Jurassic coalfield were accumulated in the shores of shallow lakes and are characterized by relatively high S content (>1.0%) [53].

4.2. Coal Petrology

Macerals in the late Carboniferous Taiyuan Formation coals are dominated by vitrinite (avg. 69.5–79.5%), followed by inertite (20.5–29.5%), with trace amounts of liptinite (Table 1). Those in the early Permian Shanxi Formation coals are also dominated by vitrinite, but coals from the Weibei Carboniferous-Permian coalfield are also characterized by higher vitrinite and lower inertinite contents compared to those from the Shanbei Carboniferous-Permian coalfield.

The Late Triassic Nos. 3 and 5 coals consist mainly of vitrinite (77.5–76.2%), and to a lesser extent inertite (22.3–23.4%), with trace liptinite content (<1.0%). The Middle Jurassic coals generally contain relatively higher inertite contents ranging from 26.55% to 55.21%; vitrinite contents in the Middle Jurassic coals range from 44.7% to 72.5% (Table 1).

Table 1. Proximate analysis results and maceral contents for the studied coals from the main coal fields in Shaanxi Province.

Coal Seam	Coalfield	Coal Mine	M, ad%	A, d%	V, daf%	St, d%	Vitrinite, %	Inertinite, %	Liptinite, %		
Carboniferous-Permian	Taiyuan Formation (C _{2t})	No. 5	Jinghuashan (JHS)	0.1–0.3 (0.2)	7.1–33.0 (19.6)	15.7–27.5 (19.4)	0.7–3.6 (1.8)	76.4	23.5	0.1	
		No. 5	Dongdong (DD)	0.3–0.5 (0.4)	7.6–30.6 (18.1)	15.8–25.5 (19.7)	1.1–9.7 (3.8)	79.5	20.5	0.00	
		No. 5	Xiangshan (XS)	0.9–1.5 (1.2)	11.5–36.2 (19.0)	15.3–19.5 (16.6)	0.3–5.6 (2.2)	71.9	27.9	0.2	
		No. 11	Sangshuping (SSP)	0.5–2.2 (1.0)	8.1–22.7 (14.8)	13.2–27.8 (16.3)	3.0–8.4 (4.6)	69.5	29.5	1.0	
	Shanxi Formation (P _{1s})	No. 3	Sangshuping (SSP)	Weibei Carboniferous-Permian (C-P)	0.6–3.1 (1.2)	7.4–21.0 (12.1)	13.7–18.3 (16.2)	0.3–0.5 (0.4)	70.5	28.7	0.8
		No. 4	Puran (PR)	Shanbei Carboniferous-Permian (C-P)	1.8–2.9 (2.4)	15.3–45.0 (26.4)	38.7–41.9 (40.8)	0.2–0.4 (0.2)	61.2	38.1	0.7
Late Triassic	Wayaobao Formation (T _{3w})	No. 3	Yongming (YM)	Shanbei Triassic	1.2–1.6 (1.5)	2.8–25.2 (9.2)	35.2–39.0 (37.3)	0.4–0.5 (0.5)	77.5	22.3	0.2
		No. 5			1.3–1.7 (1.5)	6.7–38.4 (19.8)	36.4–44.6 (42.2)	0.3–0.8 (0.6)	76.2	23.4	0.5
Middle Jurassic	Yanan Formation (J _{2y})	No. 3	Zhangjiawa (ZJW)	Shanbei Jurassic	2.9–4.4 (3.4)	6.7–26.7 (7.4)	34.9–46.3 (39.8)	1.2–4.1 (1.8)	47.0	52.0	1.0
		No. 1	Chuijiagou (CJG)		6.8–8.5 (7.3)	2.0–5.1 (3.9)	30.5–39.1 (34.6)	0.2–0.8 (0.4)	57.0	42.7	0.3
		No. 2			5.1–7.0 (5.8)	2.3–21.9 (7.4)	37.9–47.0 (40.7)	0.3–0.5 (0.3)	72.5	26.6	0.9
		No. 3	Huanglong Jurassic	5.5–6.3 (6.0)	1.8–4.8 (3.1)	32.7–41.6 (36.9)	0.3–0.8 (0.3)	70.2	27.7	2.1	
		No. 4		Dafoshi (DFS)	3.1–3.6 (3.4)	7.0–17.4 (9.4)	29.1–38.9 (32.3)	0.1–0.2 (0.1)	44.7	55.2	0.1
		No.4		Chenjiashan (CJS)	3.1–5.0 (4.0)	6.7–26.7 (14.0)	30.7–41.0 (35.2)	0.2–0.3 (0.2)	51.4	47.8	0.9

ad, air dry basis; d, dry basis; daf, dry and ash free basis.

The variation of maceral composition and proportion in coals from different coal fields and different geological ages are largely influenced by the subsidence rate of basin basement and the marine transgression process. Due to the slow subsidence in the northern area, in addition to the marine transgression from southwest to northeast of the late Carboniferous-early Permian epicontinental basin in North China, relatively oxidized raised bog was more readily formed in the northern area, which is close to the sediment source. This finding is also evidenced by the aforementioned obviously lower volatile matter yield of Carboniferous-Permian coals in the northern area with respect to the southern area, which is in accordance with a previous study that showed the vitrinite reflectance of coals of the same geological age decreases from south to north due to the multiple effects of tectonism and the subsidence rate [54].

4.3. Coal Mineralogy

4.3.1. Carboniferous-Permian Coals

Mineral Composition

Minerals in the late Carboniferous Taiyuan Formation coals (No. 5 and No. 11) from the Weibei C-P Coalfield consist mainly of kaolinite (avg. 38.0–70.0%, on an ash basis, which was recalculated using the ash yield values of the studied samples) and calcite (avg. 21.3–35.2%, on an ash basis), with minor and different proportions of quartz, tobelite, dolomite, pyrite, siderite, ankerite, and anatase in different coal mines (Table 2). Furthermore, svanbergite, chalcopyrite, galenite, and apatite, although below the detection limit of XRD analysis, were also identified in these coals by SEM-EDS analysis, as accessory phases [6,55].

Minerals in the early Permian Shanxi Formation coals (No. 3) from the Weibei C-P Coalfield are also mainly composed of kaolinite (avg. 47.9%), calcite (avg. 17.3%), in addition to tobelite (avg. 18.2%) and ankerite (avg. 10.1%), with minor amounts of apatite and quartz. In contrast, the early Permian Shanxi Formation coals (No. 4) in the Shanbei C-P Coalfield are almost entirely composed of kaolinite (avg. 88.9%), with small proportions of calcite (avg. 8.8%) and apatite (avg. 2.5%).

Modes of Occurrence of Minerals

Generally, kaolinite occurs in various forms in the C-P coals, sometimes identified as lenticles or irregular debris along bedding planes (Figure 5a), demonstrating a terrigenous detrital origin. In some cases, kaolinite, in conjunction with goyazite (Figure 5b) or apatite (Figure 5c), is also found as infillings, presumably suggesting a co-precipitation from solutions [7,55]. In a few cases, kaolinite also occurs as cell infillings (Figure 5d), coexisting with pyrite (Figure 5e) or melanterite (Figure 5f), and to a lesser extent, epigenetic disseminated pyrite occurs on the surface of kaolinite, indicating an authigenic precipitation from solutions during syngenetic to early diagenetic stages. In addition, there was input of felsic volcanic debris during accumulation of the Late Carboniferous coals as evidenced by the presence of high temperature quartz, and zircon in coals from the Weibei coalfield [4], and vermicular kaolinite in partings of coals from the Shanbei coalfield [7]. Therefore, kaolinite could also originate from alteration of synchronous volcanic inputs.

Carbonate minerals in the studied coals, principally dolomite and calcite, occur primarily as irregular fracture infillings (Figure 6a,b), indicative of an epigenetic precipitation from solutions [13,56–58]. In some cases, particles of siderite occur as cavity infillings of kaolinite (Figure 6c), pointing to an authigenic origin [59,60]. The occurrence of euhedral particles and fracture infilling of ankerite is also indicative of an epigenetic origin (Figure 6c,d).

Pyrite is found as framboidal pyrite grains and fracture infillings (Figures 5e, 6b,c and 7a,b), respectively indicating a syngenetic and epigenetic origin for pyrite crystallization [10,16,59]. In a few instances, chalcopyrite and galenite occur in the form of cavity infillings within organic matter or kaolinite, indicating authigenic precipitation (Figure 7c,d).

Table 2. Semi-quantitative mineral composition of coals from the Weibei and Shanbei C-P coal fields in Shaanxi Province as deduced from XRD analysis (% , on ash basis).

	Coalfield	Coal Mine	Qtz	Kln	Cal	Dol	Sd	Ank	Py	Tb	Gp	Ant	Ap	
C _{2t}	Weibei	No. 5	JHS	<dl-16.9 (5.1)	2.3–92.7 (41.4)	<dl-93.4 (35.2)	<dl-22.7 (6.0)	<dl-4.2 (1.0)	<dl	<dl-15.5 (4.4)	<dl-48.1 (6.9)	<dl	<dl	
		No. 5	DD	<dl-7.2 (0.8)	1.4–83.6 (38.0)	<dl-72.9 (25.4)	<dl-11.7 (4.8)	<dl-6.6 (1.5)	<dl	<dl-52.0 (19.1)	<dl-19.8 (8.8)	<dl-6.9 (1.3)	<dl-2.3 (0.2)	<dl
		No. 5	XS	<dl-0.9 (0.1)	23.9–99.1 (70.0)	<dl	<dl-6.7 (1.7)	<dl	<dl-14.8 (3.3)	<dl-65.9 (22.1)	<dl	<dl	<dl-1.0 (0.1)	<dl
		No. 11	SSP	<dl	14.8–85.4 (58.2)	<dl-77.5 (21.3)	<dl	<dl	<dl	<dl-45.0 (9.7)	<dl-20.8 (6.1)	<dl-6.4 (1.1)	<dl	<dl
P _{1s}	Weibei	No. 3	SSP	<dl-14.5 (1.6)	18.2–83.3 (47.9)	<dl-56.9 (17.3)	<dl-3.0 (0.4)	<dl	<dl-23.4 (10.1)	<dl	<dl-53.5 (18.2)	<dl	<dl	<dl-27.4 (4.5)
	Shanbei	No. 4	PR	<dl	63.1–97.8 (88.9)	<dl-36.9 (8.8)	<dl	<dl	<dl	<dl	<dl	<dl	<dl	<dl-9.3 (2.5)

Qtz, quartz; Kln, kaolinite; Cal, calcite; Dol, dolomite; Sd, siderite; Ank, ankerite; Py, pyrite; Tb, tobelite; Gp, gypsum; Ant, anatase; Ap, apatite; <dl, below XRD detection limit.

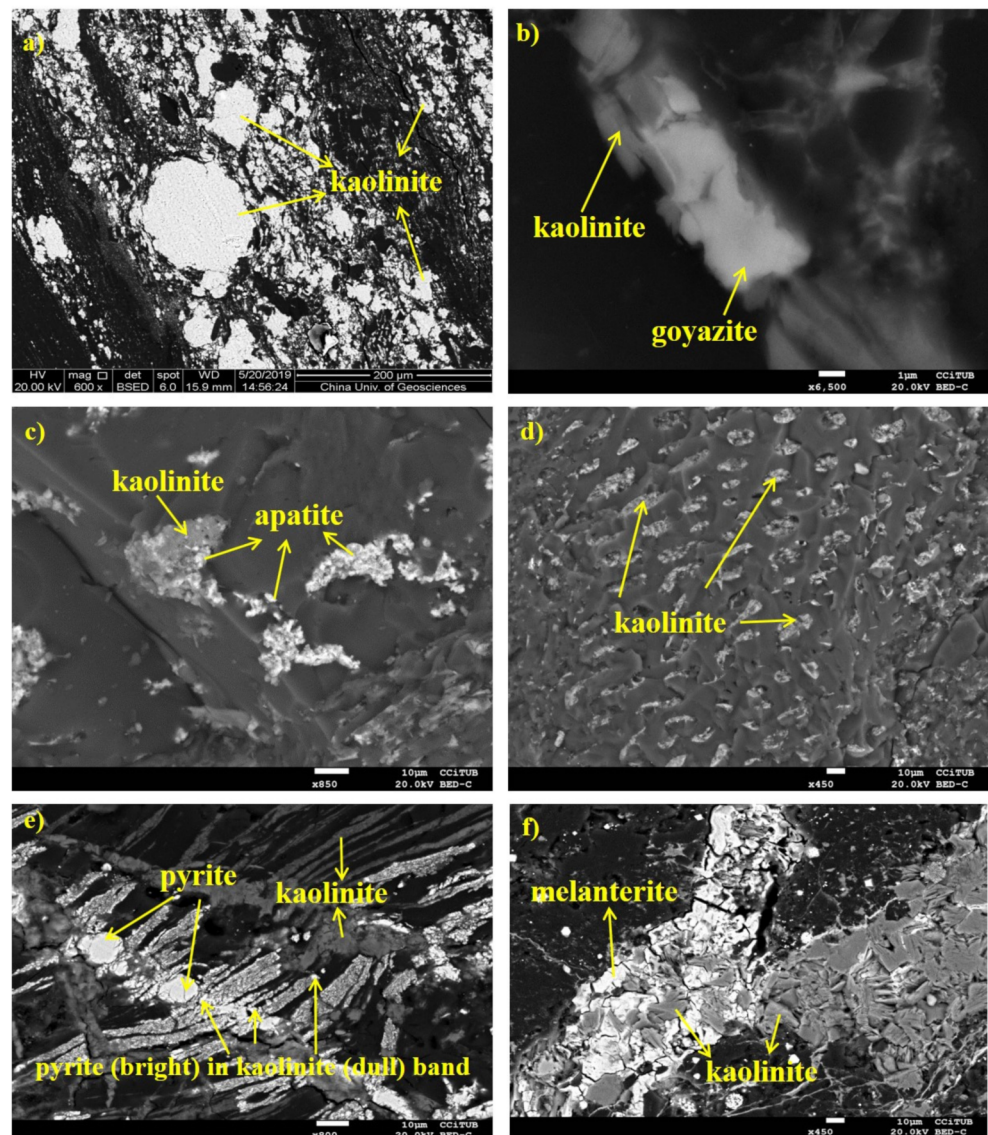


Figure 5. SEM images of kaolinite in the Carboniferous–Permian coals: (a) kaolinite lenses and debris in Puran Permian coal; (b) kaolinite intergrown with goyazite in Jinhua Shan Carboniferous coal; (c) kaolinite intergrown with apatite in Puran Permian coal; (d) fusinite infilling with kaolinite in Dongdong Carboniferous coal; (e,f), re-mineralized pyrite and melanterite in kaolinite of Sangshuping Carboniferous coal.

In addition, apatite occurs as cavity infillings within kaolinite particles (Figures 5c and 7c) and cell infillings of organic matter (Figure 8a), all of which indicates an authigenic origin. Due to the occurrence of felsic volcanic debris during accumulation of the Late Carboniferous coals, apatite is presumably originated from inputs either from synchronous volcanic or epiclastic inputs into palaeomires. Authigenic zircon also occasionally occurs as euhedral crystals in the C–P coals (Figure 8b), which is either originated from the synchronous volcanic input or detrital influx from the metamorphic or volcanic rocks in the basements. Traces of barite were found filling the cavity of organic matter (Figure 8c), or occur as cleat-filling veins (Figure 8d), representing a possible crystallization from hydrothermal fluids or Ba-rich solutions that originated from alterations of feldspars or volcanic debris.

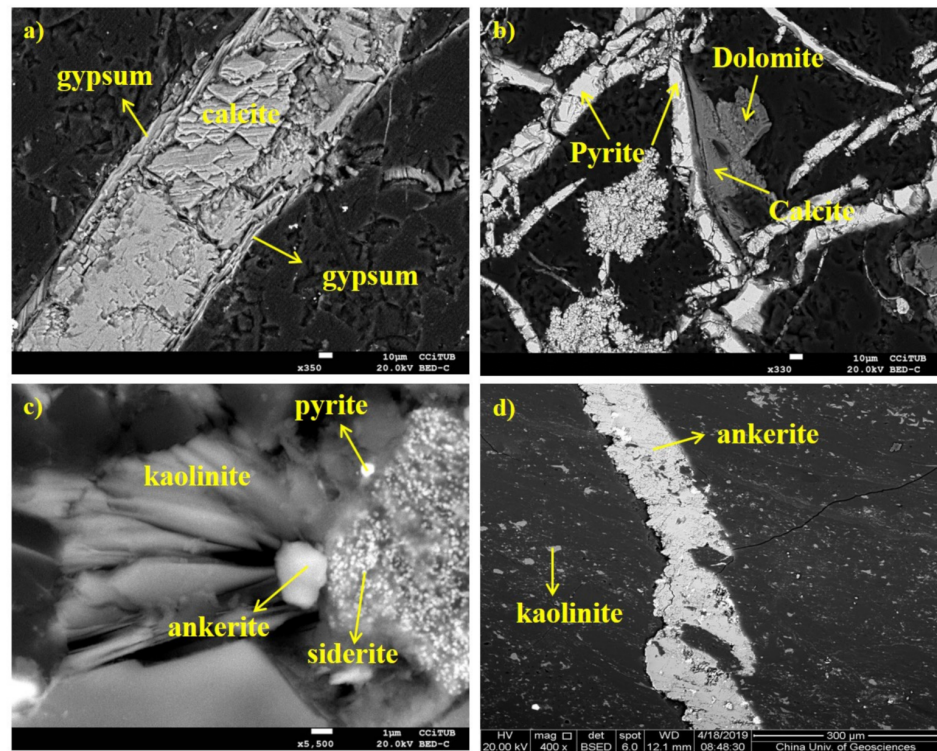


Figure 6. SEM images of carbonate minerals in the Carboniferous-Permian coals: (a) fracture-filling calcite in Sangshuping Carboniferous coal; (b) fracture-filling calcite and dolomite in Jinhuashan Carboniferous coal; (c) euhedral particles of ankerite and siderite in Xiangshan Carboniferous coal; (d) fracture-filling ankerite in Puran Permian coal.

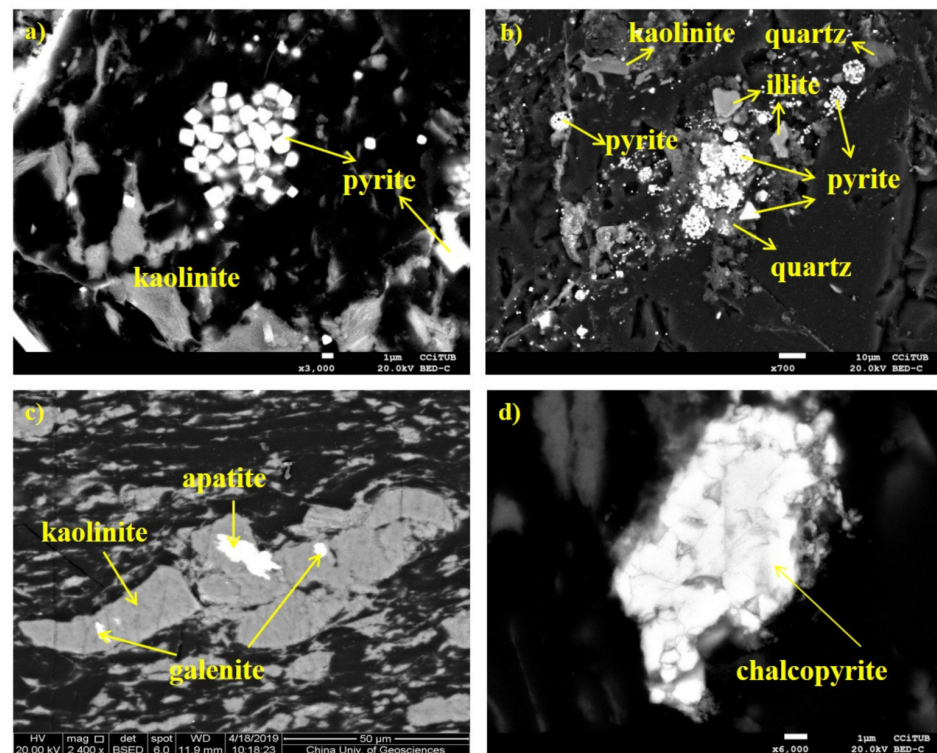


Figure 7. SEM images of carbonate minerals in the Carboniferous-Permian coals: (a,b) euhedral pyrite in Sangshuping Carboniferous coal; (c) cavity infilling of galenite in Puran Permian coal; (d) cavity infilling of chalcopyrite in Dongdong Carboniferous coal.

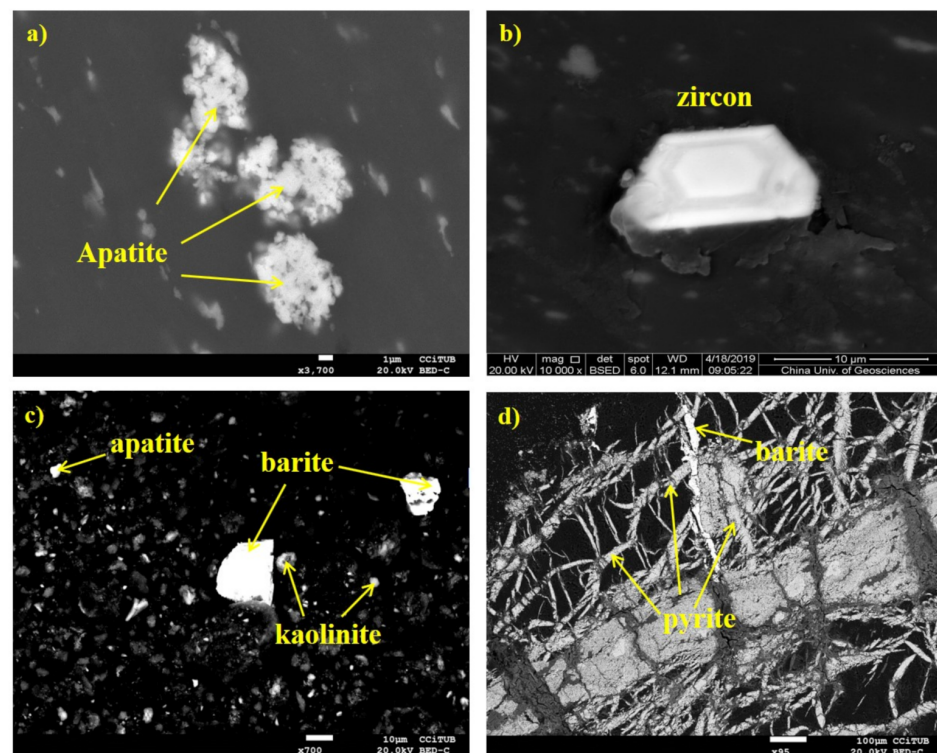


Figure 8. SEM images of heavy minerals in the Carboniferous-Permian coals. (a) microcrystals of apatite in Dongdong Carboniferous coal; (b) euhedral zircon in Puran Permian coal; (c) barite particles in Puran Permian coal; (d) cleating-filling barite veins in Jinhuaashan Carboniferous coal.

Vertical Distribution of Minerals

The contents and composition of minerals remarkably varies in different coal seams of the Taiyuan Formation and Shanxi Formation in the Weibei C-P coal fields. In the Taiyuan Formation No. 11 coal from the Sangshuping coal mine, kaolinite and tobelite are higher in abundance in the middle and lower portion, whereas pyrite and gypsum occur only in the roof and upper portion of the coal seam (Figure 9). Microcline was only detected in the coal partings (Figure 9). In the Taiyuan Formation No. 5 coal from the Xiangshan coal mine, kaolinite and illite are the dominant minerals and present an inverse distribution along the coal seam; the former is higher in abundance in the upper portion, whereas the latter is mainly higher in the lower portion (Figure 10), probably due to the variation in the clastic influx ratio or the source of detritic material during the peat accumulation process, or due to the alteration of kaolinite by hydrothermal solutions. Dolomite, pyrite, and ankerite occur in the middle and lower portion (Figure 10). As reported by Li et al. (2020b) [55], in the Taiyuan Formation No. 5 coal from the Jinhuaashan coal mine, calcite, dolomite, siderite, pyrite, and tobelite are higher in abundance in the lower portion, decreasing towards the upper part (Figure 11). Dolomite and siderite have a similar distribution, possibly indicating a similar origin. The parting contains higher quartz, kaolinite, and illite compared to the coals, and tobelite occurs only in the bottom of the coal seam (Figure 11). In the Taiyuan Formation No. 5 coal from the Dongdong coal mine, kaolinite is relatively low in the middle and upper parts and increases towards the lower parts (Figure 12). However, calcite has an inverse distribution to that of kaolinite. Pyrite is a ubiquitous constituent throughout the No. 5 coal but is higher in the upper parts. Tobelite is commonly identified in the middle and lower coal benches and presents a similar distribution to kaolinite (Figure 12). Siderite is abundant in the middle coal benches but appears to disappear in the upper and lower coal benches. Quartz is only found in the upper coal benches. The parting (DD-5-13P) contains higher kaolinite and tobelite content.

In the Shanxi Formation No. 4 coal from the Puran coal mine (Shanbei C-P coal field), kaolinite displays an increasing tendency from the lower to the upper portion. Calcite is found in the top and bottom coal benches but is below the detection limit in the middle coal benches. Fluorapatite is only identified in the middle coal benches (Figure 13).

In the Shanxi Formation No. 3 coal from the Sangshuping coal mine, kaolinite also displays an increasing tendency from the lower to upper part (Figure 14). Calcite content is higher in the upper portion and bottom coal benches but is lower in the middle coal benches. Quartz occurs in the top coal benches, whereas ankerite and tobelite occurs in the middle and lower portion. Fluorapatite is only identified in a few coal samples in the lower coal benches (Figure 14).

4.3.2. Triassic Coals

The minerals in the late Triassic Wayaobao Formation mainly comprise quartz (avg. 36.9–45.1%, on ash basis) and kaolinite (avg. 39.8–43.8%) (Table 3). In addition, a minor proportion of calcite was identified in the lower coal benches of the No. 3 coal, and traces of illite and albite were only found in sample YM3-2. Minor amounts of calcite, siderite, ankerite, and pyrite, in addition to traces of illite and albite, are present in the No. 5 coal (Figure 15).

Quartz and kaolinite have similar distribution patterns in the No. 3 coal (Table 3), possibly indicating a similar source. In the No. 5 coal, the distribution of pyrite is similar to that of ankerite, and calcite content decreases from the bottom to top of the No. 5 coal and is absent from the parting (Figure 15), possibly because the non-coal rock has a low permeability and keeps Ca-rich solutions percolating into the parting.

In the late Triassic coals, kaolinite is found as cleat or fracture infillings, intimately with calcite and pyrite (Figure 16a–c), indicating an epigenetic origin. Calcite was also found in the coals as fusinite cell-fillings or co-existing with kaolinite (Figure 16d–f), indicating an authigenic origin and its formation after kaolinite.

4.3.3. Jurassic Coals

Mineral Composition

The minerals in the No. 3 coal from the Zhangjiawa coal mine and the Nos. 1, 2, and 3 coals from the Cuijiagou coal mine in the Shanbei coalfield consist mainly of quartz (avg. 31.3–81.7%, on an ash basis), calcite (avg. 1.2–46.6%), and kaolinite (avg. 6.1–21.1%), in addition to minor amounts of pyrite, ankerite, dolomite, gypsum, and jarosite identified in different coal seams. It is worth noting that the minerals in the No. 3 coal from the Cuijiagou mine are dominated by quartz (up to 81.7% on average), with a minor proportion of kaolinite (avg. 15.8%), and traces of calcite, pyrite, and gypsum.

The minerals in the No. 4 coal from the Dafoshi and Chenjiashan coal mines in the Huanglong coalfield are composed mainly of quartz (avg. 35.4–45.1%), calcite (avg. 20.5–31.5%), and kaolinite (avg. 13.5–28.4%), with minor proportions of siderite (avg. 0.5% in the Chenjiashan mine and 16.1% in the Dafoshi mine), ankerite (3.6% in the Dafoshi mine), dolomite (3.3% in the Chenjiashan mine), and fluorapatite (2.1% in the Chenjiashan mine).

Mineral Distribution

In the Zhangjiawa coal mine, quartz and kaolinite have a similar vertical distribution in the No. 3 coal, indicating a similar geological control (Figure 17). However, calcite has an inverse distribution to kaolinite, which is most likely because the coal benches rich in kaolinite and quartz have low permeability, which keeps Ca-rich fluids permeating into the coal. Pyrite appears to be randomly distributed across the coal seam. Gypsum occurs in the lower portion and jarosite is observed only in the lower coal bench (Figure 17).

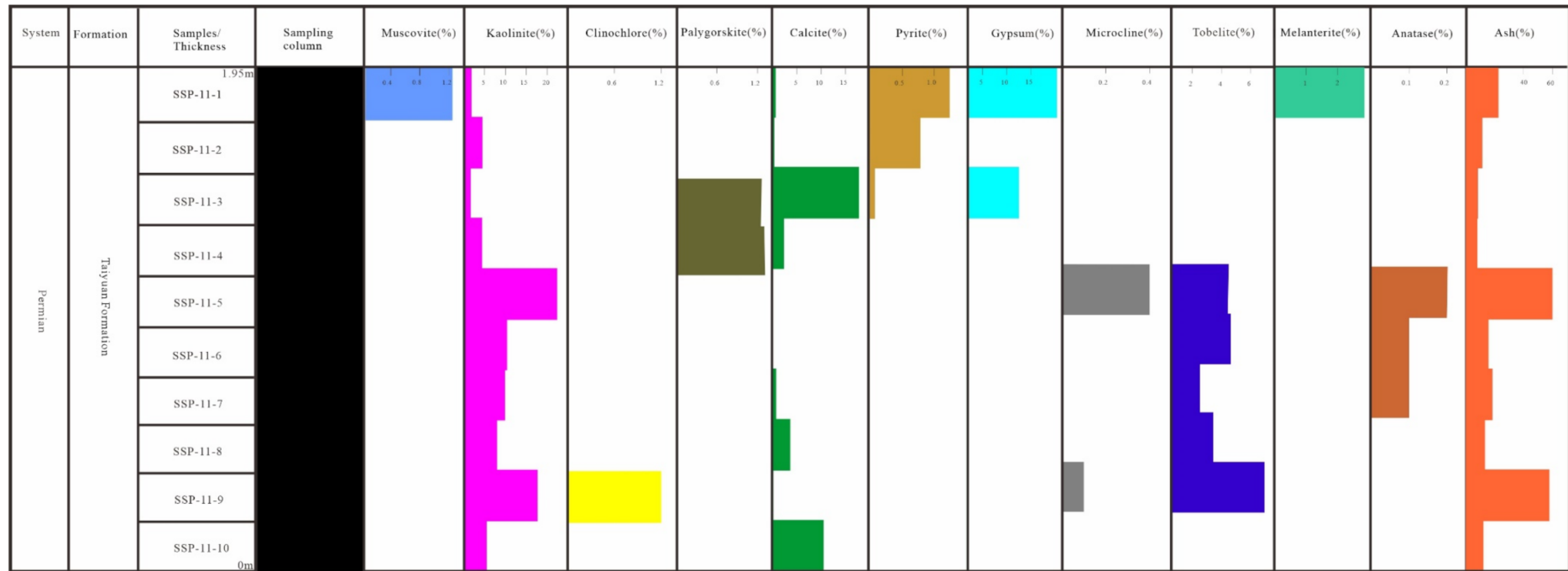


Figure 9. Vertical variations of minerals through the No. 11 coal section in the Sangshuping coal mine of the Weibei Carboniferous-Permian coalfield.

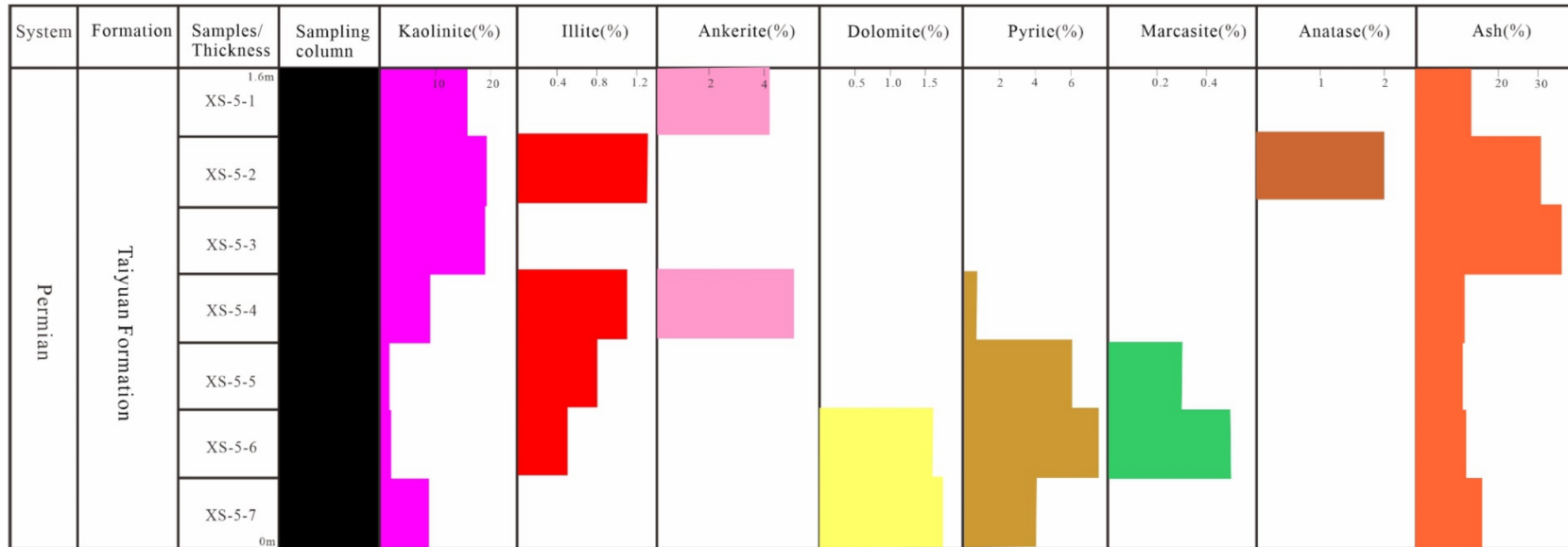


Figure 10. Vertical variations of minerals through the No. 5 coal section in the Xiangshan coal mine of the Weibei C-P coalfield.

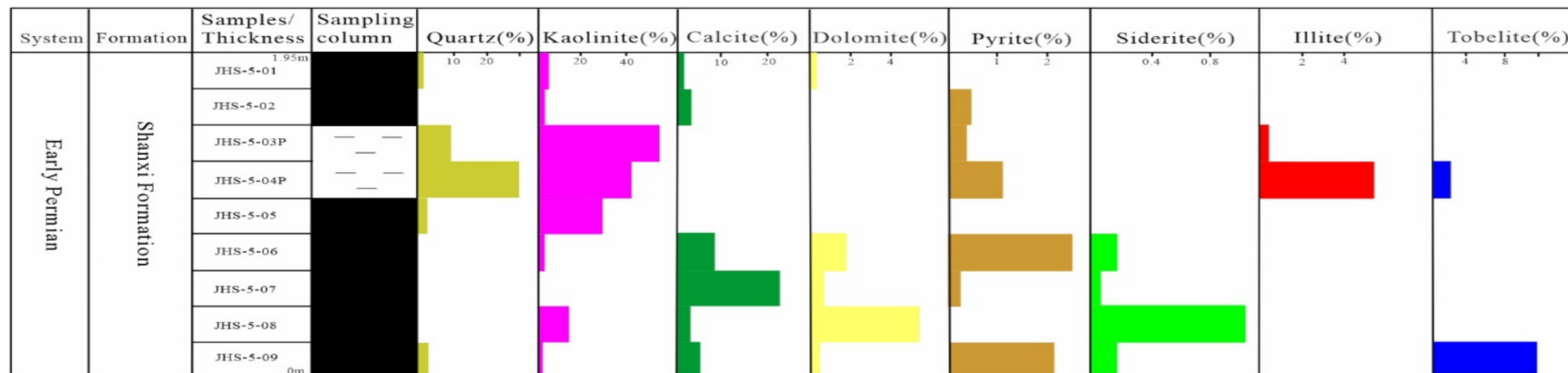


Figure 11. Vertical variations of minerals through the No. 5 coal section in the Jinghuashan coal mine of the Weibei C-P coalfield.

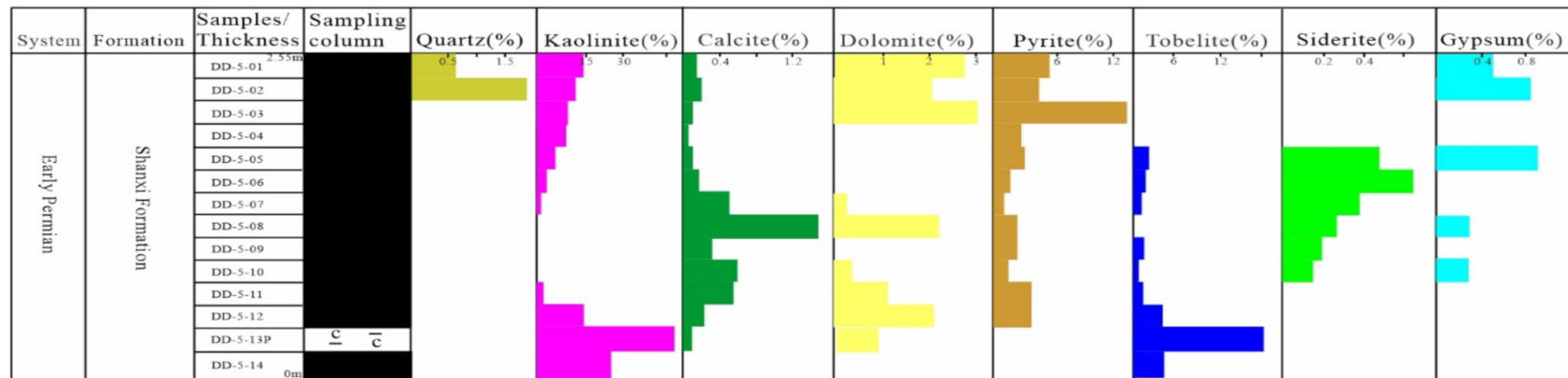


Figure 12. Vertical variations of minerals through the No. 5 coal section in the Dongdong coal mine of the Weibei C-P coalfield.

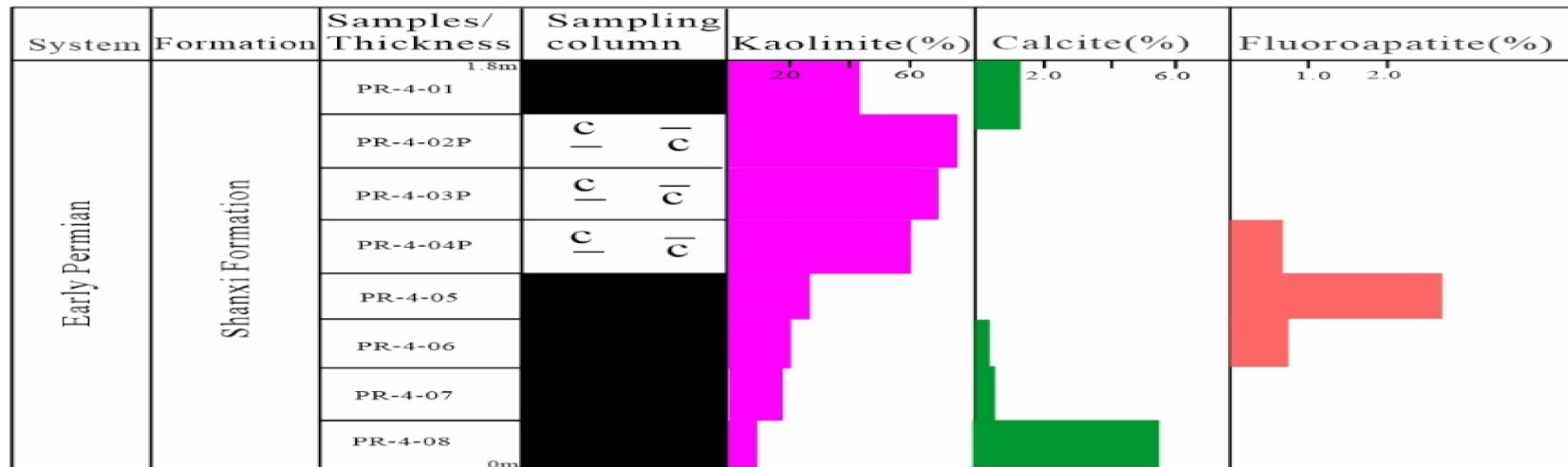


Figure 13. Vertical variations of minerals through the No. 4 coal section in the Puran coal mine of the Shanbei C-P coalfield.

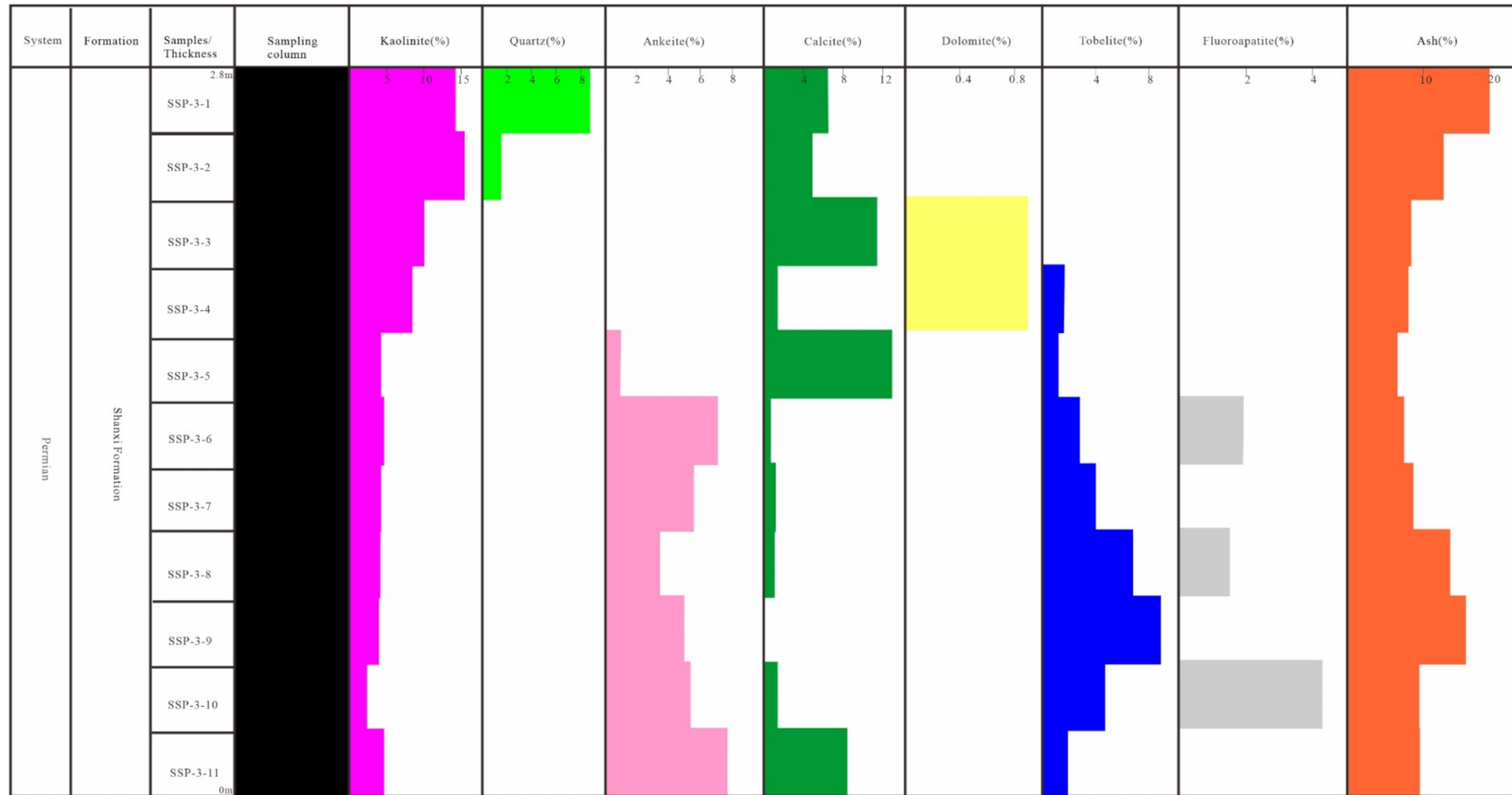


Figure 14. Vertical variations of minerals through the No. 3 coal section in the Sangshuping coal mine of the Weibei C-P coalfield.

Table 3. Semi-quantitative mineral composition of coals from the Triassic and Jurassic coal fields in Shaanxi Province as deduced from XRD analysis (% on ash basis).

	Coalfield	Coal Mine	Qtz	Kln	Cal	Dol	Sd	Ank	Py	Ill	Ab	Gp	F-Ap	Jar	
T _{3w}	No. 3	Shanbei Triassic	YM	23.2–59.8 (45.1)	35.5–57.1 (43.8)	<dl-19.6 (9.7)	<dl	<dl	<dl	<dl-0.8 (0.2)	<dl-1.2 (0.3)	<dl	<dl	<dl	
	No. 5			18.2–57.0 (36.9)	28.1–57.0 (39.7)	<dl-27.3 (9.4)	<dl	<dl-34.9 (9.5)	<dl-9.4 (2.6)	<dl-4.3 (1.5)	<dl-2.6 (0.4)	<dl-1.2 (0.2)	<dl	<dl	<dl
J _{2y}	No. 1	Shanbei Jurassic	CJG	11.4–59.5 (31.3)	5.7–44.4 (20.0)	<dl-82.9 (46.6)	<dl	<dl	<dl	<dl-6.3 (0.8)	<dl	<dl-2.1 (0.3)	<dl	<dl	
	No. 2			<dl-92.0 (34.2)	<dl-100 (21.1)	<dl-85.0 (36.5)	0.0–1.3 (0.1)	<dl-27.7 (3.2)	<dl-15.0 (3.4)	<dl-4.8 (1.2)	<dl	<dl	<dl-4.3 (0.6)	<dl	<dl
	No. 3			70.6–96.2 (81.7)	3.8–29.4 (15.8)	<dl-7.1 (1.2)	<dl	<dl	<dl	<dl-2.6 (0.8)	<dl	<dl	<dl-2.6 (0.4)	<dl	<dl
	No. 3		ZJW	3.0–63.3 (32.8)	<dl-21.8 (6.1)	2.6–90.9 (41.9)	<dl	<dl	<dl	1.7–74.6 (15.0)	<dl	<dl	<dl-14.1 (3.6)	<dl	<dl-8.5 (0.7)
	No. 4		DFS	13.6–55.9 (35.4)	4.7–23.8 (13.5)	4.4–69.9 (31.5)	<dl	1.2–29.4 (16.1)	<dl-16.0 (3.6)	<dl	<dl	<dl	<dl	<dl	<dl
No. 4	Huanglong Jurassic	CJS	8.2–66.3 (45.1)	7.1–53.3 (28.4)	0.4–76.7 (20.5)	<dl-25.3 (3.3)	<dl-4.3 (0.5)	<dl	<dl	<dl	<dl	<dl	<dl-14.1 (2.1)	<dl	

Qtz, quartz; Kln, kaolinite; Cal, calcite; Dol, dolomite; Sd, siderite; Ank, ankerite; Py, pyrite; Ill, illite; Ab, albite; Gp, gypsum; Jrs, jarosite; F-Ap, Fluorapatite <dl, below XRD detection limit.

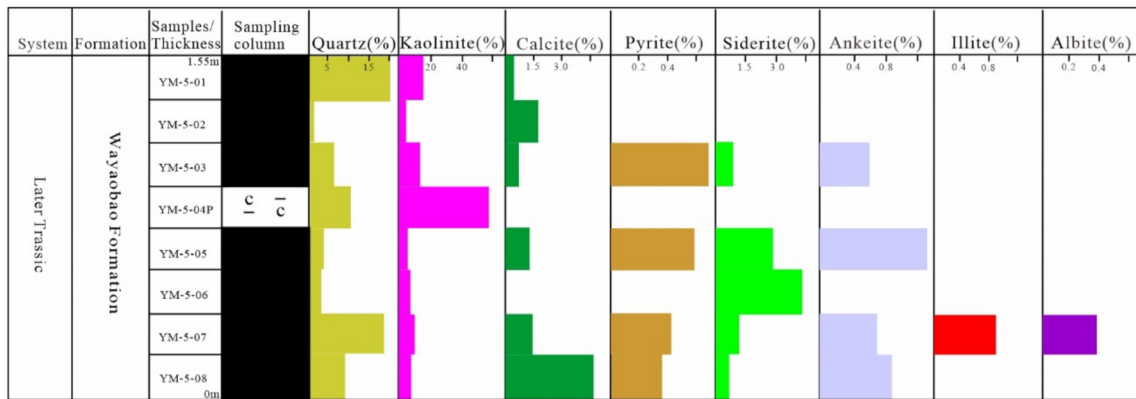


Figure 15. Vertical variations of minerals through the No. 5 coal section in the Yongming coal mine of the Shanbei Triassic coalfield.

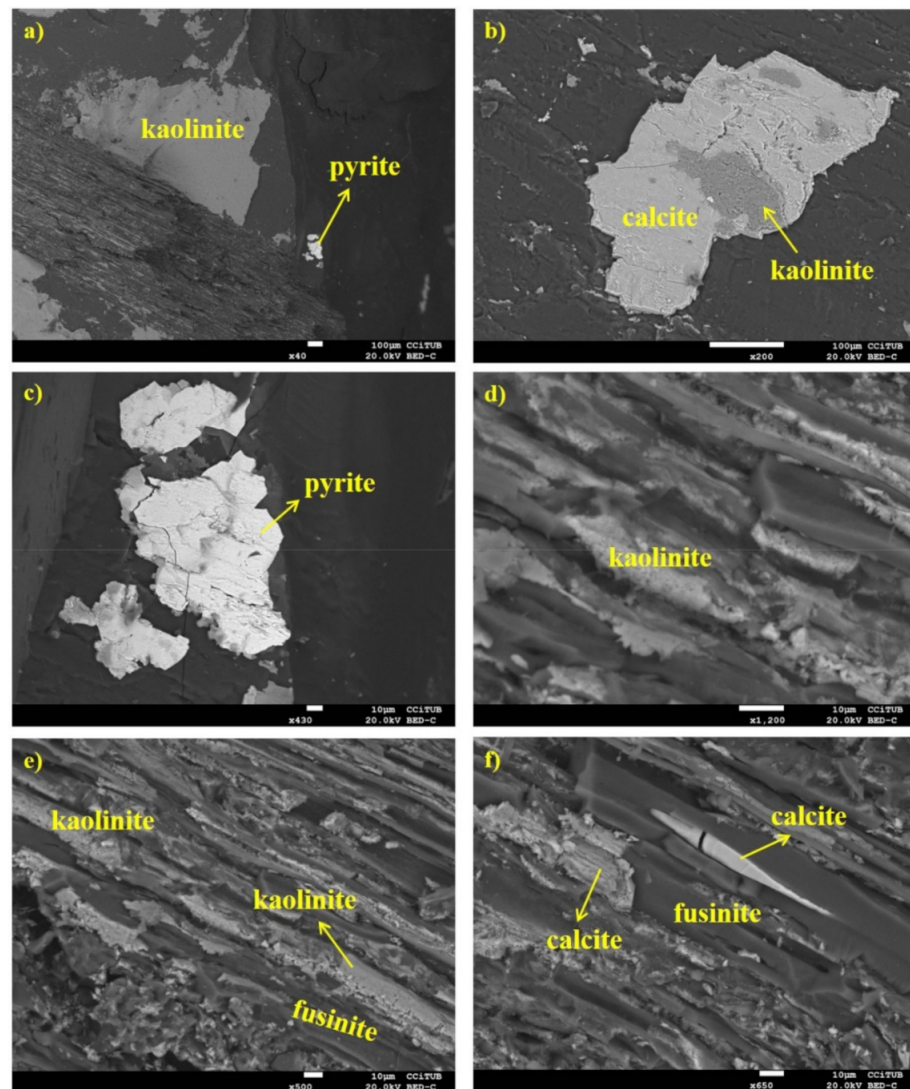


Figure 16. SEM images of minerals occurring in the late Triassic coals: (a–c) cleat infillings of kaolinite, pyrite, and calcite in the Yongming Triassic coal; (d–f) cell infillings of kaolinite and calcite in fusinite of the Yongming Triassic coal.

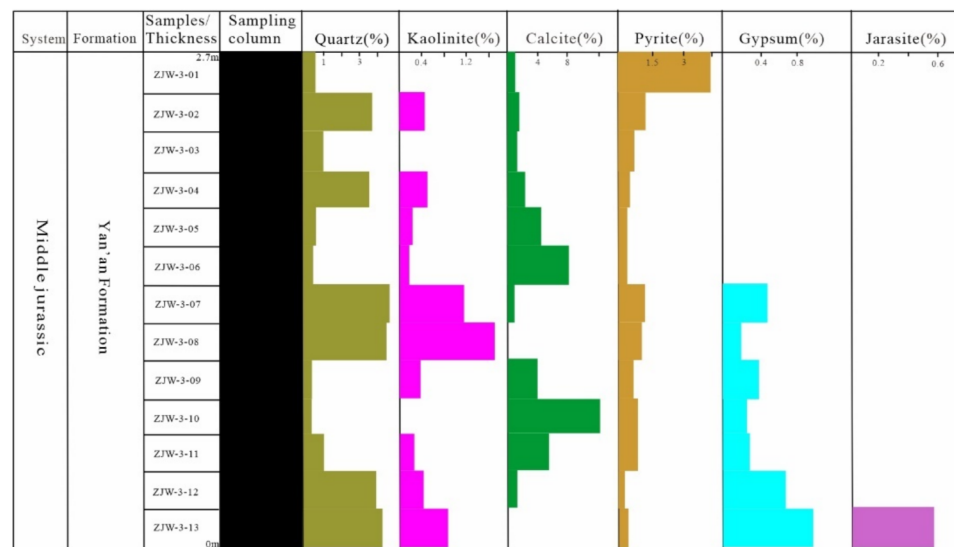


Figure 17. Vertical variations of minerals through the No. 3 coal section in the Zhangjiawa coal mine from the Shanbei Jurassic coalfield.

In the Cuijiagou coal mine, quartz and kaolinite have a similar distribution and totally decrease towards the upper part of the No. 1 coal seam (Figure 18); calcite occurs in the middle and upper portion but is below the XRD detection limit in the bottom coal benches; pyrite and gypsum only occur in the top of coal bench. In the No. 2 coal seam, quartz and kaolinite are rich in the middle and lower coal benches but calcite is rich in the upper coal benches through the coal section (Figure 19); pyrite, siderite, and gypsum are only observed in the middle coal benches; dolomite and ankerite are present in the top or upper part of coal seam. In the No. 3 coal seam, quartz is concentrated in the upper and lower coal benches but kaolinite is rich in the middle coal benches; calcite, gypsum, and pyrite are only randomly present in a few coal benches (Figure 20).

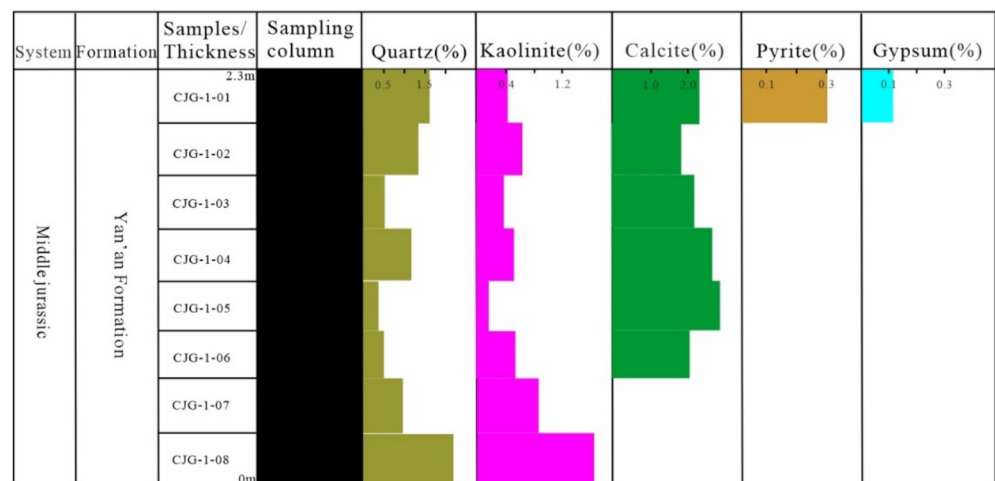


Figure 18. Vertical variations of minerals through the No. 1 coal section in the Chuijiagou coal mine from the Shanbei Jurassic coalfield.

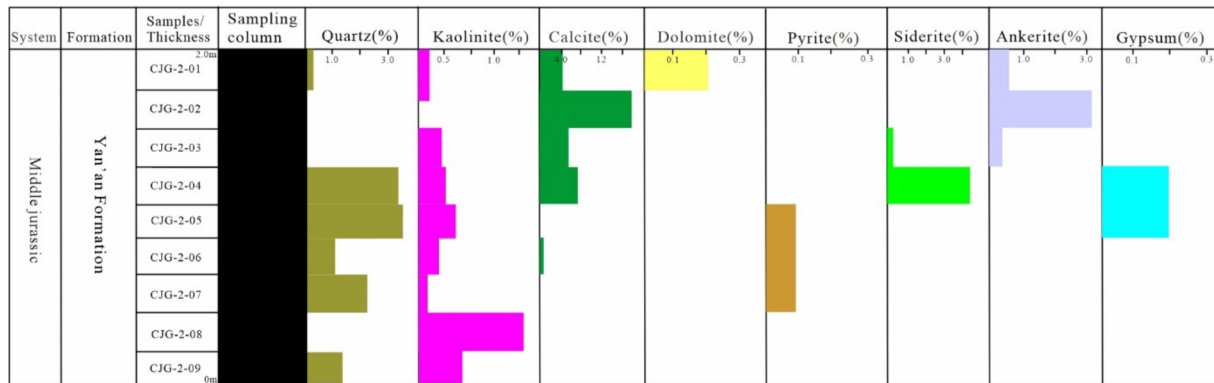


Figure 19. Vertical variations of minerals through the No. 2 coal section in the Chuijiagou coal mine of the Shanbei Jurassic coalfield.

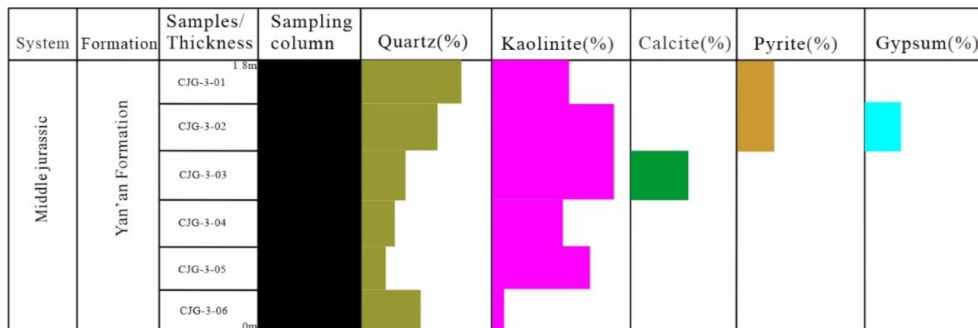


Figure 20. Vertical variations of minerals through the No. 3 coal section in the Chuijiagou coal mine of the Shanbei Jurassic coalfield.

In the Dafoshi coal mine, quartz, kaolinite, and siderite have a similar distribution through the No. 4 coal section; calcite and ankerite have a similar distribution, which is the reverse of that of quartz (Figure 21). By contrast, in the Chenjiashan coal mine, quartz and kaolinite also have similar distribution tendencies along the No. 4 coal section, which are similar to that of the ash yield; calcite and dolomite also present a similar distribution, with higher contents in the middle coal benches; fluorapatite and siderite occur in the upper coal benches (Figure 22).

Modes of Occurrence of Minerals

SEM-EDS shows that euhedral calcite and ankerite occur mainly as cell infillings, pointing to an authigenic origin (Figure 23a,b), and in a few cases, calcite is present as euhedral particles (Figure 23c). Euhedral barite crystal is observed filling the cavities of calcite (Figure 23d). Kaolinite occurs as massive particles and cavity infillings within organic matter, and occasionally coexists with fluorapatite (Figure 23e). Fluorapatite also occurs as cleat infillings (Figure 23f), representing an epigenetic origin. Quartz is present as irregular particles along the bedding planes (Figure 23e), or as cavity infillings within organic matter (Figure 23f,g), indicative of both a detrital and authigenic origin. Sphalerite occurs as inclusions within the calcite (Figure 23b), demonstrating its formation prior to calcite. Euhedral pyrite particles are precipitated on the surface of calcite (Figure 23c), or distributed along the fractures as cavity infillings within organic matter (Figure 23g), both reflecting an epigenetic origin for its formation. In some cases, gypsum is found occurring as fracture infillings, which indicates an epigenetic origin (Figure 23h), and rutile occasionally occurs as finely dispersed particles within organic matter (Figure 23e).

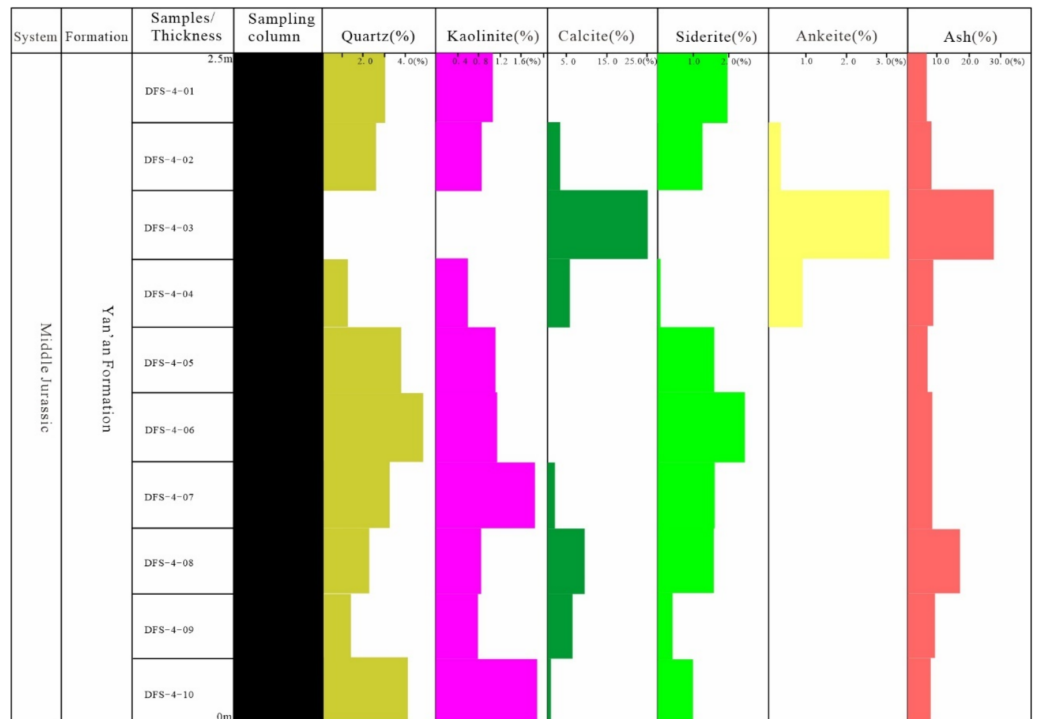


Figure 21. Vertical variations of minerals through the No. 4 coal section in the Dafoshi coal mine of the Huanglong Jurassic coalfield.

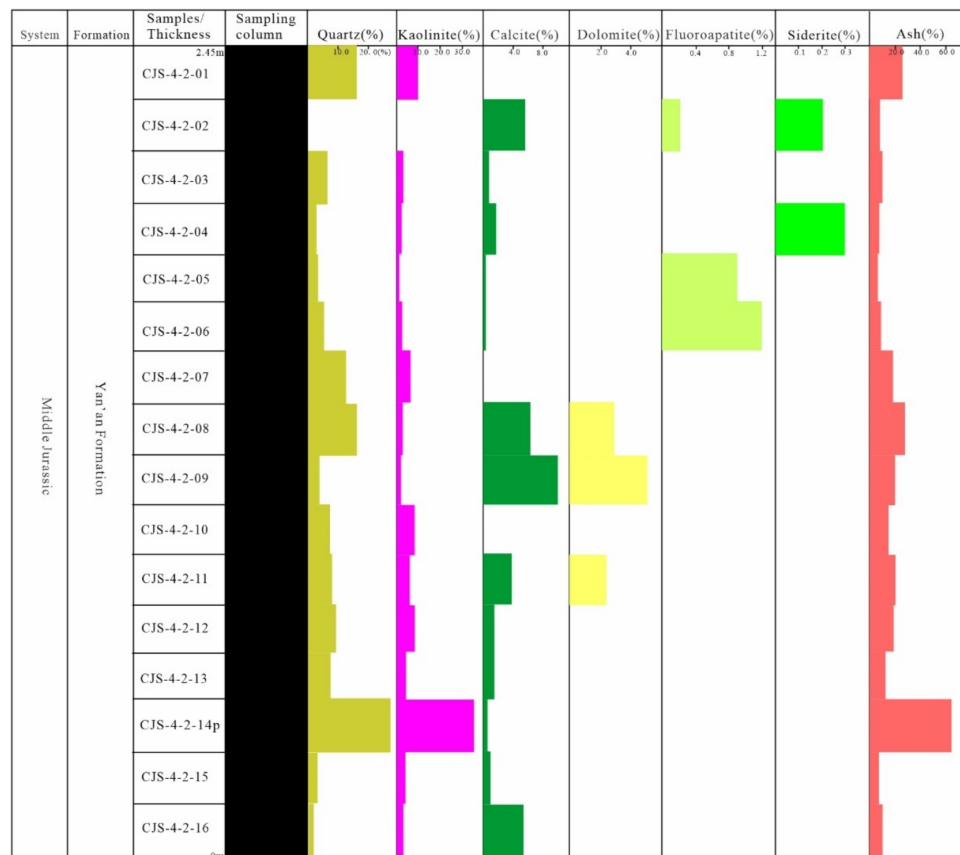


Figure 22. Vertical variations of minerals through the No. 4 coal section in the Chenjiasan coal mine of the Huanglong Jurassic coalfield.

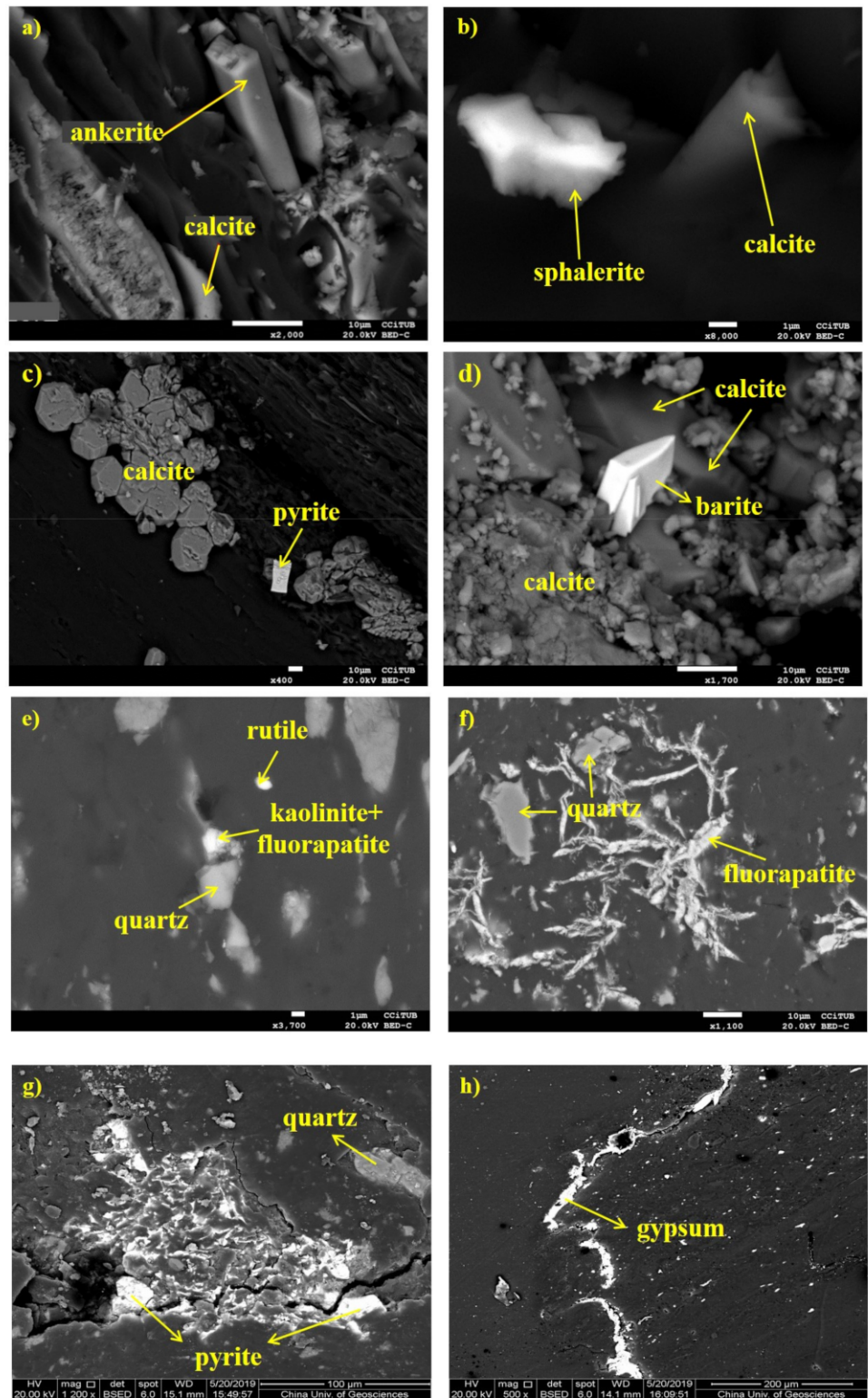


Figure 23. SEM images of minerals occurring in the middle Jurassic coals: (a) cell-filling ankerite and calcite particles in Dafoshi Jurassic coal; (b) euhedral sphalerite and calcite in Dafoshi Jurassic coal; (c) crystals of calcite and pyrite in Cuijiagou Jurassic coal; (d) euhedral barite in the Zhangjiawa Jurassic coal; (e) syngenetic microcrystals of fluorapatite, rutile, and kaolinite in the Chenjiashan Jurassic coal; (f) cleat infilling of fluorapatite in the Chenjiashan Jurassic coal; (g,h) fracture infilling of pyrite and gypsum in the Cuijiagou Jurassic coal.

5. Discussion

5.1. Origins of Typical Minerals in Different Coals

5.1.1. Clay Minerals

Kaolinite is the most common clay mineral occurring in all the coal seams in Shaanxi. The various modes of occurrence of kaolinite in coals indicates different origins for its formation. Those occurring in the form of lenticles and thin layers were inherited from the source rocks, representing a terrigenous detrital origin. Those cell-, fracture-, and cleat-filling kaolinites are of authigenic origins, which were formed by interaction of weathered source rocks with syngenetic or epigenic fluids.

Tobelite is ubiquitously present in coals from the Weibei C-P coal field [6,55]. As previously mentioned, tobelite is a high-temperature hydrothermal indicator, usually occurring in high-rank coals, and has also been found present in several Permo-Carboniferous coals in China [60–62]. The well-developed fault structure and associated high-temperature hydrothermal activities in the Weibei coalfield evidenced that tobelite in coals originated from hydrothermal alteration of kaolinite with the active participation of NH_4^+ from organic matter at a relatively high temperature.

5.1.2. Carbonate Minerals

Carbonate minerals, e.g., calcite, dolomite, ankerite, and siderite, are the main minerals in the Shaanxi coals, especially in the Permo-Carboniferous and Jurassic coals. In most cases, calcite and dolomite occur in the form of irregular fracture infillings (Figure 6b), indicative of an epigenetic precipitation from solutions. In some cases, euhedral calcite and ankerite occur as cell infillings (Figures 16f and 23a), and in a few cases, calcite is present as massive particles (Figure 23c), pointing to an authigenic origin. However, the cell-filling calcite and its coexistence with kaolinite indicate a later formation stage because palaeomire is commonly acidic condition which hampers the formation of calcite during syngenetic to early diagenetic stages. In contrast, particles of siderite occur as cavity infillings of kaolinite (Figure 6c), indicating a syngenetic origin, which is in consonance with previous research showing that siderite was commonly formed by authigenic precipitation during the syngenetic to early diagenetic stage [10,59,63].

5.2. Change in Mineral Assemblages with Different Coal Fields and Geological Ages

The composition, proportions, and assemblages of minerals remarkably vary in different coal fields of different geological ages. Minerals in the late Carboniferous-early Permian coals are dominated by kaolinite and calcite (Figure 24), due to the co-effect of terrigenous/volcanic debris influx and paralic sedimentary environment. The late Carboniferous-early Permian coal-bearing strata in North China was formed on the long-term weathering basement of the Ordovician [40], and there was occasionally an input of felsic volcanic debris during accumulation of the Late Carboniferous coals [4,7], which provided abundant detrital influx for kaolinite precipitation [14,17]. Furthermore, the late Carboniferous-early Permian coal-bearing strata in North China was deposited in an epicontinental marine-influenced environment, which gave rise to the high sulfur content [10,64]. Due to the rapid tectonic subsidence rate of the basement and the relatively abundant provenance system during the formation of the late Triassic coals, minerals in the Wayaobao Formation coals are mainly composed of quartz and kaolinite (Figure 24). In comparison, the middle Jurassic coals were formed in confined lacustrine sedimentary environment with a relatively slow basement subsidence rate, and minerals in them are dominantly composed of quartz and calcite (Figure 24), with a minor proportion of kaolinite.

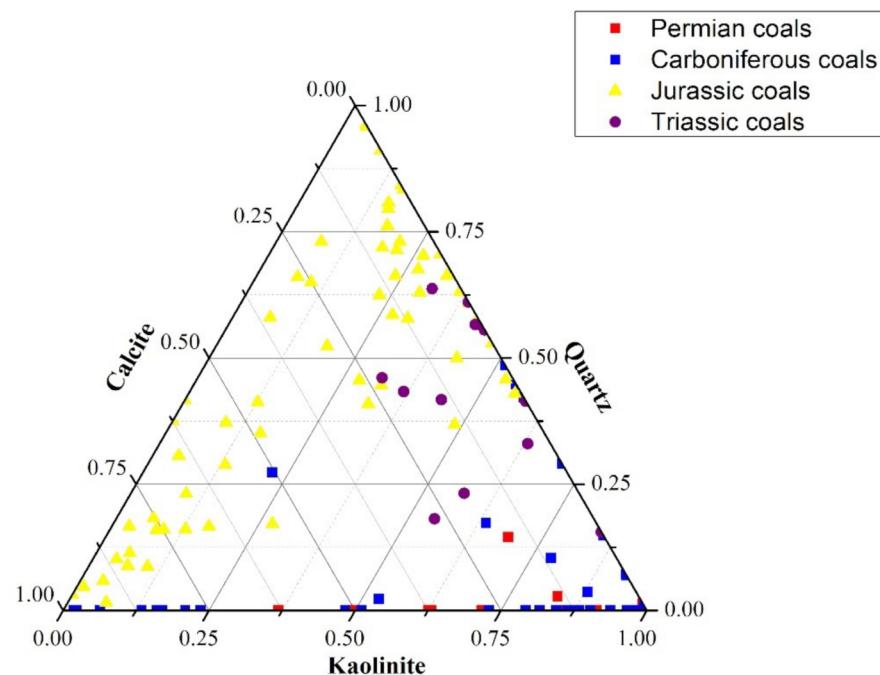


Figure 24. Ternary plots of principle mineral compositions in coals of different geological ages.

Formed in the same geological age, coals deposited in different parts of the coal basin have different mineral characteristics. For instance, the Shanxi Formation coals from the Shanbei C-P coalfield in the north of Shaanxi Province are characterized by higher kaolinite and lower carbonate (calcite, dolomite, and ankerite) contents compared to those from the Weibei C-P coalfield in the south of Shaanxi Province, and tobelite occurs in coals from the Weibei C-P coalfield rather than the Shanbei C-P coalfield. With respect to the Taiyuan Formation No. 5 coals from the Weibei C-P coal field, the quartz content decreased and pyrite content increased northwards from the Jinhuaashan to Dongdong to Xiangshan coal mine (Table 2). With respect to the Jurassic coals, those from the Shanbei Jurassic coalfield in the north have different proportions of pyrite and gypsum, whereas those from the Huanglong Jurassic coalfield have minor amount of fluorapatite.

5.3. Geological Controls on Mineralogical Characteristic Differences

The geological controls on minerals in coals commonly include terrigenous material input, seawater invasion, volcanic ash fall, igneous intrusion, descending and ascending groundwater, chemical compositions of groundwater, influence of hydrothermal solutions and/or chemistry of circulating porewaters [13,15,56]. In the present research, the aforementioned differences in mineral contents, compositions, and assemblages in different coal fields of different geological ages are primarily influenced by the sedimentary settings (including seawater invasion, tectonic setting, subsidence, and buried rate) and terrigenous detrital input from sedimentary provenance, in addition to the intrusion of hydrothermal fluids.

5.3.1. Influence of Sedimentary Setting

The peat-forming environment is to a large extent controlled by the sedimentary settings during accumulation of the coal-bearing sequences. Coal-bearing sequences of the late Carboniferous were deposited during the epicontinental transitional sedimentary period, during which the coal was highly influenced by seawater and terrigenous clastics, with a relatively high buried rate and low degree of oxidation and decomposition. As a consequence, the Taiyuan Formation coals are commonly characterized by relatively high sulfur, high vitrinite, and high pyrite contents. During the early seawater transgression stage, the Taiyuan Formation No. 11 coal was formed in the lagoon-tidal flat environment

on a confined carbonate platform and developed only in the Sangshuping coal mine in the northeastern corner of the Weibei C-P coal field. It is characterized by super-high organic sulfur content and relatively low pyrite content, similar to that of some Late Permian SHOS coals in southern China that are formed in tidal flat environments on restricted carbonate platforms [15,65–69]. As the seawater transgression further proceeded during the second and the upper member of the Taiyuan Formation, the Taiyuan Formation No. 5 coals were widely developed in the Weibei C-P coal field. Due to the sufficient iron supply, sulfur in the No. 5 coals occurs predominantly in the form of pyritic sulfur, with high pyrite content.

The Triassic coals were formed during the late filling stage of a large inland lake basin, and accordingly characterized by relatively high vitrinite and mineral contents with low sulfur and pyrite contents. The Jurassic coals were deposited in similar sedimentary settings to the Triassic coals, but with low terrigenous detrital supply, giving rise to low mineral contents. As previously mentioned, different proportions of pyrite, gypsum, and jaracite occur in the Shanbei Jurassic coals and sulfur content in some of the Shanbei Jurassic coals are relatively high. These tiny differences were ascribed to the low influence of terrigenous clastics during formation of the Shanbei Jurassic coals, which were formed in a relatively occlusive confined lake sedimentary environment.

5.3.2. Influence of Terrigenous Detrital Input

Terrigenous detrital input from sedimentary provenance also plays a significant role in coal mineralogical characteristics. During the Late Paleozoic, the sediment source for the North China block is, to a large degree, mainly from the Yinshan Oldland [70]. However, the Weibei C-P coalfield and Huanglong Jurassic coalfield are situated on the southwestern edge of North China, where the sediment source for the Late Paleozoic strata is controversial. It was reported that during the Late Paleozoic, the sediment source for the southcentral part of the North China block and the Ordos basin was controlled by detrital supplies from both the Yinshan tectonic belt to the north and the Central China Orogenic Belt (including Qinling, Dabie, Qilian, and Kunlun Mountain Ranges) to the south [6,60,71]. In the Weibei C-P coal field, quartz content in the Taiyuan Formation No. 5 coals increased southwards from the Xiangshan to Dongdong to Jinhushan coal mine, probably due to the relatively high influence of terrigenous clastics from Qinling-Qilian Oldland, which is characterized by abundant quartz and lithoclast contents [6,72].

During deposition of the Shanxi Formation, the northern margin of the Ordos Basin was the Alxa Uplift and Yinshan Uplift, and the southern margin was the Qilian Uplift and North Qinling Uplift. With the exception that the northern areas close to the Alxa and Yinshan Uplift, which belong to inland piedmont clastic coal-bearing sequences, the remaining areas belong to open basin clastic coal-bearing sequences. As a consequence, due to the higher influence of terrigenous detrital inputs originating from the Yinshan Oldland, which is rich in feldspar and mica but poor in quartz in composition, the Shanxi Formation coals in the Shanbei C-P coalfield are characterized by higher ash yields and mineral contents relative to those in the Weibei C-P coalfield, with minerals dominated by kaolinite. Furthermore, relative to the north part of the Ordos Basin, the subsidence rate was much higher in the south part during this period, which gave rise to higher coal rank (low volatile bituminous) of the Shanxi Formation coal from the Weibei C-P coalfield.

During the deposition period of the Jurassic Yan'an Formation, due to the northward push from the Qinling-Qilian orogenic belt, the uplift was stronger in the south than in the north, and coal-bearing strata of the Yan'an Formation were mainly composed of coarse clastic rocks in the south and fine clastic rocks in the north [73]. Consequently, the Huanglong Jurassic coals in the south present relatively higher ash yields and mineral contents due to the stronger terrigenous inputs of coarse clastic rocks from the southern provenance.

5.3.3. Influence of Hydrothermal Fluids

The mineral assemblages of coals from different coal fields and different geological ages are to a large extent influenced by multiple hydrothermal activities during and after the coalification stage. As discussed above, several minerals, e.g., calcite, dolomite, pyrite, and occasionally chalcopyrite and barite in the studied coals, are confirmed as occurring primarily as fracture and cleat infillings (Figures 5–8, 16 and 23), which is indicative of epigenetic hydrothermal activities [56,58,66,73,74].

Furthermore, kaolinite occurs in various forms in the studied coals; some fracture or cleat infilling of kaolinite in the Shanbei Jurassic coals also evidenced the epigenetic input of hydrothermal fluids [7]. However, it is more common that kaolinite occurs as cell or pore space infillings in the Weibei and Shanbei C-P coals, which precipitated from syngenetic fluid derived from the weathered source region. The occurrence of apatite as cell infillings of organic matter (Figure 8a) and cavity infillings within kaolinite particles (Figure 7c) also indicated the input of syngenetic hydrothermal fluid.

In addition to the fracture and cleat infilling minerals, the ubiquitous occurrence of tobelite in the Weibei C-P coalfield is most likely caused by the hydrothermal activities, although this was not observed by SEM-EDX [6,55]. In particular, the Shanxi Formation coals from the Weibei C-P coalfield present much high calcite content than those from the Shanbei C-P coalfield; other carbonate minerals (dolomite and ankerite), in addition to tobelite, are also present in coals from the Weibei C-P coalfield, but were not detected in the coals from the Shanbei C-P coalfield. In addition, fracture-infilling pyrite also occurs in tobelite-bearing samples (Figures 6b and 8d). This may indicate that the Shanxi Formation coals from the Weibei C-P coalfield experienced much stronger influences of other more hydrothermal fluids than those forming fracture- and cleat-infilling calcite in coals from the Shanbei C-P coalfield. The presence of tobelite along with fracture-infilling minerals (e.g., pyrite or quartz) in coal is commonly indicative of high temperature (>200 °C) hydrothermal activities [75–78]. It has been confirmed that tectonic activities were intensive in the Weibei C-P coalfield, with a well-developed folding structure in the west and faulting structures intensely developed in the east [79]. The fault structures played a key role in the movement and migration of hydrothermal fluids towards coal seams during the syngenetic and epigenetic process, which highly influenced the mineralogical and geochemical characteristics of coals. Furthermore, the high temperature hydrothermal fluids along with the rapid subsidence rate also led to the high coal rank in the Weibei C-P coalfield, as indicated by the relatively low volatile matter yield and high vitrinite reflectance [54].

6. Conclusions

The late Carboniferous Taiyuan Formation, the early Permian Shanxi Formation, the late Triassic Wayaobao Formation, and the middle Jurassic Yan'an Formation are the main coal-bearing sequences in the Shaanxi Province. The Permo-Carboniferous coals, the late Triassic coals, and the middle Jurassic coals are respectively characterized by medium-high, low-medium, and low ash yields, which indicates that they were respectively formed in lowland bog, medium bog, and highland bog environments. Coals from the Weibei C-P coalfield belong to low volatile bituminous whereas coals from other coalfields belong to high volatile bituminous.

Vitrinite is the dominant maceral in the Permo-Carboniferous coals, with an increasing tendency from the north (the Shanbei C-P coal field) to the south (the Weibei C-P coal field), probably due to the slow subsidence in the northern area and the marine transgression from the southwest towards the northeast of the Permo-Carboniferous epicontinental basin in North China. The late Triassic coals are also mainly composed of vitrinite, whereas the middle Jurassic coals are characterized by much higher inertinite content, which is also ascribed to the fast subsidence rate and peat burying rate during the late Triassic period.

The minerals in the late Carboniferous-early Permian coals are mainly composed of kaolinite and calcite, whereas those in the late Triassic coals are dominated by quartz and

kaolinite, and those in the middle Jurassic coals are dominated by quartz and calcite, with relatively high kaolinite content. These different mineral assemblages in coals of different geological ages are controlled by integrated influences of differential terrigenous detrital input, sedimentary settings, sea transgression and regression processes, and hydrothermal activities.

Author Contributions: Conceptualization, W.Y. and J.L.; methodology, W.Y.; investigation, W.Y., J.L., G.Y., L.P.; writing—original draft preparation, W.Y.; writing—review and editing, J.L. and X.Z.; supervision, X.Z.; and project administration, J.L. and X.Z. All authors have read and agreed to the published version of the manuscript.

Funding: The research was supported by the National Science Foundation of China (Nos. 41972179, 41972180), the National Key R&D Program of China (No. 2018YFF0215400), the Fundamental Research Funds for the Central Universities, China University of Geosciences (Wuhan) (No. CUGCJ1819).

Acknowledgments: The authors express great gratitude to the editors and anonymous reviewers for their comments to improve the manuscript.

Conflicts of Interest: The authors declare no conflict of interest.

References

1. Lv, J.; Zhao, Y. Characteristic Analysis of Elements in Coal in Huanglong Jurassic Coalfield. *Coal Geol. China* **2015**, *27*, 15–18.
2. Bai, G.; Liu, X.; Fan, Z.; Li, X. Epidemiologic survey on coal-burning endemic arsenism in Shaanxi Province. *Chin. J. Endem.* **2006**, *25*, 57–60.
3. Luo, K.; Ren, D.; Xu, L.; Dai, S.; Cao, D.; Feng, F.; Tan, J. Fluorine content and distribution pattern in Chinese coals. *Int. J. Coal Geol.* **2004**, *57*, 143–149. [[CrossRef](#)]
4. Wang, X.; Dai, S.; Ren, D.; Yang, J. Mineralogy and geochemistry of Al-hydroxide/oxyhydroxide mineral-bearing coals of Late Paleozoic age from the Weibei coalfield, southeastern Ordos Basin, North China. *Appl. Geochem.* **2011**, *26*, 1086–1096. [[CrossRef](#)]
5. Zhang, X.; Wu, H.; Li, W. Analysis of coal reserves in Shaanxi Province. *Inn. Mong. Coal Econ.* **2015**, *6*, 200–210.
6. Li, J.; Wu, P.; Yang, G.; Pan, L.; Zhuang, X.; Querol, X.; Moreno, N.; Li, B.; Shangguan, Y. Enrichment of Li–Ga–Zr–Hf and Se–Mo–Cr–V–As–Pb Assemblages in the No. 11 Superhigh Organic Sulfur Coal from the Sangshuping Coal Mine, Weibei Coalfield, Shaanxi, North China. *Energies* **2020**, *13*, 6660. [[CrossRef](#)]
7. Shangguan, Y.; Zhuang, X.; Li, J.; Li, B.; Querol, X.; Liu, B.; Moreno, N.; Yuan, W.; Yang, G.; Pan, L.; et al. Geological Controls on Mineralogy and Geochemistry of the Permian and Jurassic Coals in the Shanbei Coalfield, Shaanxi Province, North China. *Minerals* **2020**, *10*, 138. [[CrossRef](#)]
8. Brownfield, M.E.; Affolter, R.H.; Stricker, G.D.; Hildebrand, R.T. High chromium contents in Tertiary coal deposits of northwestern Washington—A key to their depositional history. *Int. J. Coal Geol.* **1995**, *27*, 153–169. [[CrossRef](#)]
9. Querol, X.; Whateley, M.; Fernandez-Turiel, J.-L.; Tuncali, E. Geological controls on the mineralogy and geochemistry of the Beypazari lignite, central Anatolia, Turkey. *Int. J. Coal Geol.* **1997**, *33*, 255–271. [[CrossRef](#)]
10. Ward, C.R. Analysis and significance of mineral matter in coal seams. *Int. J. Coal Geol.* **2002**, *50*, 135–168. [[CrossRef](#)]
11. Yudovich, Y.E.; Ketris, M.P. *Inorganic Matter of Coal*; Urals Branch of RAS: Ekaterinburg, Russia, 2002; p. 422.
12. Spears, D. The origin of tonsteins, an overview, and links with seatearths, fireclays and fragmental clay rocks. *Int. J. Coal Geol.* **2012**, *94*, 22–31. [[CrossRef](#)]
13. Dai, S.; Ren, D.; Chou, C.-L.; Finkelman, R.B.; Seredin, V.V.; Zhou, Y. Geochemistry of trace elements in Chinese coals: A review of abundances, genetic types, impacts on human health, and industrial utilization. *Int. J. Coal Geol.* **2012**, *94*, 3–21. [[CrossRef](#)]
14. Dai, S.; Ward, C.R.; Graham I/French, D.; Hower, J.C.; Zhao, L.; Wang, X. Altered volcanic ashes in coal and coal-bearing sequences: A review of their nature and significance. *Earth Sci. Rev.* **2017**, *175*, 44–74. [[CrossRef](#)]
15. Dai, S.; Ji, D.; Ward, C.R.; French, D.; Hower, J.C.; Yan, X.; Wei, Q. Mississippian anthracites in Guangxi Province, southern China: Petrological, mineralogical, and rare earth element evidence for high-temperature solutions. *Int. J. Coal Geol.* **2018**, *197*, 84–114. [[CrossRef](#)]
16. Dai, S.; Bechtel, A.; Eble, C.F.; Flores, R.M.; French, D.; Graham, I.T.; Hood, M.M.; Hower, J.C.; Korasidis, V.A.; Moore, T.A.; et al. Recognition of peat depositional environments in coal: A review. *Int. J. Coal Geol.* **2020**, *219*, 103383. [[CrossRef](#)]
17. Finkelman, R.B.; Dai, S.; French, D. The importance of minerals in coal as the hosts of chemical elements: A review. *Int. J. Coal Geol.* **2019**, *212*, 103251. [[CrossRef](#)]
18. Çelik, Y.; Karayıgıt, A.I.; Oskay, R.G.; Kayseri-Özer, M.S.; Christanis, K.; Hower, J.C.; Querol, X. A multidisciplinary study and palaeoenvironmental interpretation of middle Miocene Keles lignite (Harmancık Basin, NW Turkey), with emphasis on syngenetic zeolite formation. *Int. J. Coal Geol.* **2021**, *237*, 103691. [[CrossRef](#)]
19. Karayıgıt, A.I.; Bircan, C.; Oskay, R.G.; Türkmen, I.; Querol, X. The geology, mineralogy, petrography, and geochemistry of the MioceneDursunbey coal within fluvio-lacustrine deposits, Balıkesir (Western Turkey). *Int. J. Coal Geol.* **2020**, *228*, 103548. [[CrossRef](#)]

20. Liu, S.; Ma, W.; French, D.; Tuo, K.; Mei, X. Sequential Mineral Transformation during Underground Coal Gasification with the Presence of Coal Partings. *Int. J. Coal Geol.* **2019**, *208*, 1–11. [[CrossRef](#)]
21. Dai, S.; Finkelman, R.B.; French, D.; Hower, J.C.; Graham, I.T.; Zhao, F. Modes of occurrence of elements in coal: A critical evaluation. *Earth-Sci. Rev.* **2021**, *222*, 103815. [[CrossRef](#)]
22. Finkelman, R.B.; Palmer, C.A.; Wang, P. Quantification of the modes of occurrence of 42 elements in coal. *Int. J. Coal Geol.* **2018**, *185*, 138–160. [[CrossRef](#)]
23. Goodarzi, F. Assessment of elemental content of milled coal, combustion residues, and stack emitted materials: Possible environmental effects for a Canadian pulverized coal-fired power plant. *Int. J. Coal Geol.* **2006**, *65*, 17–25. [[CrossRef](#)]
24. Wang, C.; Liu, H.; Zhang, Y.; Zou, C.; Anthony, E.J. Review of arsenic behavior during coal combustion: Volatilization, transformation, emission and removal technologies. *Prog. Energy Combust. Sci.* **2018**, *68*, 1–28. [[CrossRef](#)]
25. Seredin, V.V.; Dai, S. Coal deposits as potential alternative sources for lanthanides and yttrium. *Int. J. Coal Geol.* **2012**, *94*, 67–93. [[CrossRef](#)]
26. Hower, J.C.; Qian, D.; Briot, N.; Henke, K.R.; Hood, M.M.; Taggart, R.K.; Hsu-Kim, H. Rare earth element associations in the Kentucky State University stoker ash. *Int. J. Coal Geol.* **2018**, *189*, 75–82. [[CrossRef](#)]
27. Finkelman, R.B.; Orem, W.; Castranova, V.; A Tatu, C.; Belkin, H.; Zheng, B.; E Lerch, H.; Maharaj, S.V.; Bates, A.L. Health impacts of coal and coal use: Possible solutions. *Int. J. Coal Geol.* **2002**, *50*, 425–443. [[CrossRef](#)]
28. Finkelman, R.B.; Tian, L. The health impacts of coal use in China. *Int. Geol. Rev.* **2017**, *60*, 579–589. [[CrossRef](#)]
29. Lu, X. Characteristics of environmental geochemistry of Se in Coals of Shaanxi province. *J. Shaanxi Norm. Univ.* **2003**, *31*, 107–112.
30. Luo, K.; Wang, W.; Yao, G.; Duanmu, H.; Mi, J.; Zhang, H. Sulfur content of permo-carboniferous coal and its geneses in Hancheng mine. *J. Xi'an Univ. Sci. Technol.* **2000**, *20*, 289–292.
31. Mi, J.; Ren, J.; Wang, J.C.; Bao, W.R.; Xie, K.C. Ultrasonic and Microwave Desulfurization of Coal in Tetrachloroethylene. *Energy Sources Part A Recovery Util. Environ. Eff.* **2007**, *29*, 1261–1268. [[CrossRef](#)]
32. Yang, Z.Y.; Wang, S.T.; Tan, C.; Li, Y.H. Desulfurization Effect of High-Sulfur Weibei Coal of Assisted by Microwave Irradiation and Ultrasonic Wave. *Adv. Mater. Res.* **2014**, *1070–1072*, 501–504. [[CrossRef](#)]
33. Dai, S.; Jiang, Y.; Ward, C.; Gu, L.; Seredin, V.V.; Liu, H.; Zhou, D.; Wang, X.; Sun, Y.; Zou, J.; et al. Mineralogical and geochemical compositions of the coal in the Guanbanwusu Mine, Inner Mongolia, China: Further evidence for the existence of an Al (Ga and REE) ore deposit in the Jungar Coalfield. *Int. J. Coal Geol.* **2012**, *98*, 10–40. [[CrossRef](#)]
34. Dai, S.; Li, D.; Chou, C.-L.; Zhao, L.; Zhang, Y.; Ren, D.; Ma, Y.; Sun, Y. Mineralogy and geochemistry of boehmite-rich coals: New insights from the Haerwusu Surface Mine, Jungar Coalfield, Inner Mongolia, China. *Int. J. Coal Geol.* **2008**, *74*, 185–202. [[CrossRef](#)]
35. Dai, S.; Li, T.; Jiang, Y.; Ward, C.; Hower, J.C.; Sun, J.; Liu, J.; Song, H.; Wei, J.; Li, Q.; et al. Mineralogical and geochemical compositions of the Pennsylvanian coal in the Hailiushu Mine, Daqingshan Coalfield, Inner Mongolia, China: Implications of sediment-source region and acid hydrothermal solutions. *Int. J. Coal Geol.* **2015**, *137*, 92–110. [[CrossRef](#)]
36. Li, J.; Zhuang, X.; Yuan, W.; Liu, B.; Querol, X.; Font, O.; Moreno, N.; Li, J.; Gang, T.; Liang, G. Mineral composition and geochemical characteristics of the Li-Ga-rich coals in the Buertaohai-Tianjiashipan mining district, Jungar Coalfield, Inner Mongolia. *Int. J. Coal Geol.* **2016**, *167*, 157–175. [[CrossRef](#)]
37. Zhao, L.; Dai, S.; Nechaev, V.P.; Nechaeva, E.V.; Graham, I.T.; French, D. Enrichment origin of critical elements (Li and rare earth elements) and a Mo-U-Se-Re assemblage in Pennsylvanian anthracite from the Jincheng Coalfield, southeastern Qinshui Basin, northern China. *Ore Geol. Rev.* **2019**, *115*, 103184. [[CrossRef](#)]
38. Liang, J. Studies on Sedimentology and Sequence Stratigraphy of the Jurassic in Ordos Basin. Ph.D. Thesis, Northwest University, Xi'an, China, 2007.
39. Li, L.; Shao, L.; Li, M.; Wang, D.; Lu, J.; Li, Z.; Cheng, A. Sequence-paleogeography and coal accumulation of the upper Triassic Wayaopu Formation in Ordos basin. *J. China Coal Soc.* **2017**, *42*, 2090–2100.
40. Wang, S. *Coal Accumulating and Coal Resource Evaluation of Ordos Basin*; China Coal Industry Publishing House: Chaoyang Beijing, China, 1996; pp. 1–473.
41. ASTM Standard D3173-11. *Test Method for Moisture in the Analysis Sample of Coal and Coke*; ASTM International: West Conshohocken, PA, USA, 2011; Available online: www.astm.org (accessed on 20 September 2021).
42. ASTM Standard D3175-11. *Test Method for Volatile Matter in the Analysis Sample of Coal and Coke*; ASTM International: West Conshohocken, PA, USA, 2011; Available online: www.astm.org (accessed on 20 September 2021).
43. ASTM Standard D3174-11. Annual book of ASTM standards. In *Test Method for Ash in the Analysis Sample of Coal and Coke*; ASTM International: West Conshohocken, PA, USA, 2011; Available online: www.astm.org (accessed on 20 September 2021).
44. ASTM Standard D4239-18a. *Standard Test Method for Sulfur in the Analysis Sample of Coal and Coke Using High-Temperature Tube Furnace Combustion*; ASTM International: West Conshohocken, PA, USA, 2018; Available online: www.astm.org (accessed on 20 September 2021).
45. ASTM Standard D2492-02. Annual Book of ASTM Standards. In *Standard Test Method for Forms of Sulfur in Coal: Gaseous Fuels: Coal and Coke*; ASTM International: West Conshohocken, PA, USA, 2005; Available online: www.astm.org (accessed on 20 September 2021).
46. ASTM D2798-20. *Standard Test Method for Microscopical Determination of the Vitrinite Reflectance of Coal*; ASTM International: West Conshohocken, PA, USA, 2020; Available online: www.astm.org (accessed on 20 September 2021).

47. Chung, F.H. Quantitative interpretation of X-ray diffraction patterns of mixtures: I. Matrix flushing method for quantitative multicomponent analysis. *J. Appl. Crystallogr.* **1974**, *7*, 519–525. [[CrossRef](#)]
48. MT/T 850-2000 (China). *Classification for Moisture of Coal*; China Coal Research Institute: Beijing, China, 2000.
49. GB/T 15224.1-2010 (China). *Classification for Quality of Coal. Part 1: Ash Yield*; SAC/TC469; ASTM International: Taiyuan, China, 2010.
50. ASTM Standard D388-12. *Standard Classification of Coals by Rank*; ASTM International: West Conshohocken, PA, USA, 2012; Available online: www.astm.org (accessed on 20 September 2021).
51. Yang, Q. *The coal metamorphism in China*; China Coal Industry Publishing House: Beijing, China, 1996; pp. 1–212.
52. Chou, C.L. Sulfur in coals: A review of geochemistry and origins. *Int. J. Coal Geol.* **2012**, *100*, 1–13. [[CrossRef](#)]
53. Fan, L.; Kou, G.; Hou, F. Probe into Features and Geneses of Sulfur Content in Low-sulfur Coal of Yushen Mining Area. *Coal Geol. China* **2003**, *15*, 12–13.
54. Wang, Y.; Gao, S. The distribution of coal sorts and analysis of its geologic background in Shaanxi province. *J. Xi'an Univ. Sci. Technol.* **2003**, *23*, 400–403.
55. Li, J.; Zhuang, X.; Querol, X.; Moreno, N.; Yang, G.; Pan, L.; Li, B.; Shangguan, Y.; Pan, Z.; Liu, B. Enrichment of Nb-Ta-Zr-W-Li in the Late Carboniferous Coals from the Weibei Coalfield, Shaanxi, North China. *Energies* **2020**, *13*, 4818. [[CrossRef](#)]
56. Permana, A.K.; Ward, C.; Li, Z.; Gurba, L.W. Distribution and origin of minerals in high-rank coals of the South Walker Creek area, Bowen Basin, Australia. *Int. J. Coal Geol.* **2013**, *116–117*, 185–207. [[CrossRef](#)]
57. Karayığita, A.İ.; Mastalerz, M.; Oskaya, R.G.; Buzkan, İ. Bituminous coal seams from underground mines in the Zonguldak Basin (NW Turkey): Insights from mineralogy, coal petrography, Rock-Eval pyrolysis, and meso- and microporosity. *Int. J. Coal Geol.* **2018**, *199*, 91–112. [[CrossRef](#)]
58. Dawson, G.K.W.; Golding, S.D.; Esterle, J.S.; Massarotto, P. Occurrence of minerals within fractures and matrix of selected Bowen and Ruhr Basin coals. *Int. J. Coal Geol.* **2012**, *94*, 150–166. [[CrossRef](#)]
59. Zhao, L.; Sun, J.; Guo, W.; Wang, P.; Ji, D. Mineralogy of the Pennsylvanian coal seam in the Datanhao mine, Daqingshan Coalfield, Inner Mongolia, China: Genetic implications for mineral matter in coal deposited in an intermontane basin. *Int. J. Coal Geol.* **2016**, *167*, 201–214. [[CrossRef](#)]
60. Zhu, H.; Zhang, W.; Ning, S.; Han, L.; Deng, X. Aluminum Distribution in North China Permo-Carboniferous Coal and Its Resource Prospect. *Coal Geol. China* **2018**, *30*, 21–25+29.
61. Dai, S.; Zou, J.; Jiang, Y.; Ward, C.; Wang, X.; Li, T.; Xue, W.; Liu, S.; Tian, H.; Sun, X.; et al. Mineralogical and geochemical compositions of the Pennsylvanian coal in the Adaohai Mine, Daqingshan Coalfield, Inner Mongolia, China: Modes of occurrence and origin of diasporite, gorceixite, and ammonian illite. *Int. J. Coal Geol.* **2012**, *94*, 250–270. [[CrossRef](#)]
62. Zheng, Q.; Liu, Q.; Shi, S. Mineralogy and geochemistry of ammonianillite in intraseam partings in Permo-Carboniferous coal of the Qinshui coalfield, North China. *Int. J. Coal Geol.* **2016**, *153*, 1–11. [[CrossRef](#)]
63. Golab, A.; Ward, C.R.; Permana, A.; Lennox, P.; Botha, P. High-resolution three-dimensional imaging of coal using microfocus X-ray computed tomography, with special reference to modes of mineral occurrence. *Int. J. Coal Geol.* **2013**, *113*, 97–108. [[CrossRef](#)]
64. Karayığit, A.İ.; Littke, R.; Querol, X.; Jones, T.; Oskay, R.G.; Christanis, K. The Miocene coal seams in the Soma Basin (W. Turkey): Insights from coal petrography, mineralogy and geochemistry. *Int. J. Coal Geol.* **2017**, *173*, 110–128. [[CrossRef](#)]
65. Dai, S.; Zhang, W.; Seredin, V.V.; Ward, C.; Hower, J.C.; Song, W.; Wang, X.; Li, X.; Zhao, L.; Kang, H.; et al. Factors controlling geochemical and mineralogical compositions of coals preserved within marine carbonate successions: A case study from the Heshan Coalfield, southern China. *Int. J. Coal Geol.* **2013**, *109–110*, 77–100. [[CrossRef](#)]
66. Dai, S.; Zhang, W.; Ward, C.; Seredin, V.V.; Hower, J.C.; Li, X.; Song, W.; Wang, X.; Kang, H.; Zheng, L.; et al. Mineralogical and geochemical anomalies of late Permian coals from the Fusui Coalfield, Guangxi Province, southern China: Influences of terrigenous materials and hydrothermal fluids. *Int. J. Coal Geol.* **2013**, *105*, 60–84. [[CrossRef](#)]
67. Dai, S.; Xie, P.; Ward, C.R.; Yan, X.; Guo, W.; French, D.; Graham, I.T. Anomalies of rare metals in Lopingian super-high-organic-sulfur coals from the Yishan Coalfield, Guangxi, China. *Ore Geol. Rev.* **2017**, *88*, 235–250. [[CrossRef](#)]
68. Li, W.; Tang, Y. Characteristics of the rare earth elements in a high organic sulfur coal from Chenxi, Hunan province. *J. Fuel Chem. Technol.* **2013**, *41*, 540–549.
69. Tang, Y.; He, X.; Cheng, A.; Li, W.; Deng, X.; Wei, Q.; Li, L. Occurrence and sedimentary control of sulfur in coals of China. *J. China Coal Soc.* **2015**, *40*, 1977–1988.
70. China National Administration of Coal Geology (CNACG). *Late Paleozoic Coal Geology of North China Platform*; Shanxi Science and Technology Press: Taiyuan, China, 1997.
71. Zhu, X.-Q.; Zhu, W.-B.; Ge, R.-F.; Wang, X. Late paleozoic provenance shift in the south-central North China Craton: Implications for tectonic evolution and crustal growth. *Gondwana Res.* **2014**, *25*, 383–400. [[CrossRef](#)]
72. Wan, Y. Study on the Spatial Coupling Relation of between the Sediment Source and Diagenesis of Yanchang Formation in southern Ordos Basin. Master's Thesis, Chengdu University of Technology, Chengdu, China, 2011.
73. Dai, S.; Xie, P.; Jia, S.; Ward, C.; Hower, J.C.; Yan, X.; French, D. Enrichment of U-Re-V-Cr-Se and rare earth elements in the Late Permian coals of the Moxinpo Coalfield, Chongqing, China: Genetic implications from geochemical and mineralogical data. *Ore Geol. Rev.* **2017**, *80*, 1–17. [[CrossRef](#)]
74. Li, J.; Zhuang, X.; Querol, X.; Font, O.; Izquierdo, M.; Wang, Z. New data on mineralogy and geochemistry of high-Ge coals in the Yimin coalfield, Inner Mongolia, China. *Int. J. Coal Geol.* **2014**, *125*, 10–21. [[CrossRef](#)]

75. Boudou, J.-P.; Schimmelmann, A.; Ader, M.; Mastalerz, M.; Sebito, M.; Gengembre, L. Organic nitrogen chemistry during low-grade metamorphism. *Geochim. Cosmochim. Acta* **2008**, *72*, 1199–1221. [[CrossRef](#)]
76. Daniels, E.J.; Altaner, S.P. Inorganic nitrogen in anthracite from eastern Pennsylvania, USA. *Int. J. Coal Geol.* **1993**, *22*, 21–35. [[CrossRef](#)]
77. Nieto, F. Characterization of coexisting NH₄⁺ and K-micas in very low-grade metapelites. *Am. Miner.* **2002**, *87*, 205–216. [[CrossRef](#)]
78. Ward, C.; Corcoran, J.; Saxby, J.; Read, H. Occurrence of phosphorus minerals in Australian coal seams. *Int. J. Coal Geol.* **1996**, *30*, 185–210. [[CrossRef](#)]
79. Cheng, L.; Weibei, P.-C. Coalfield Geological Tectonic Development Control Characteristics of Groundwater. Master's Thesis, Xi'an University of Science and Technology, Xi'an, China, 2013.